

Will deep water formation collapse in the North Western Mediterranean Sea by the end of the 21st century?

Iván Manuel Parras Berrocal¹, Ruben Vazquez¹, William David CabosNarvaez², Dimitry Sein³, Oscar Alvarez Esteban⁴, Miguel Bruno Mejías⁴, and Alfredo Izquierdo⁵

¹University of Cádiz

²University of Alcalá

³Alfred Wegener Institute for Polar and Marine Research

⁴Universidad de Cádiz

⁵Universidad de Cadiz

November 23, 2022

Abstract

Deep water formation (DWF) in the North Western Mediterranean (NWMed) is a key feature of Mediterranean overturning circulation. Changes in DWF under global warming may have an impact on the regional and even on the global climate. Here we analyze the deep convection in the Gulf of Lions (GoL) in a changing climate using an atmosphere-ocean regional coupled model with a high horizontal resolution enough to represent DWF. We find that under the RCP8.5 scenario the NWMed DWF collapses by 2040-2050, leading to almost a 90% shoaling in the winter mixed layer depth by the end of the century. The collapse is mainly related to changes in sea water temperature and salinity of Modified Atlantic Water (MAW) and Levantine Intermediate Water (LIW) that strengthen the vertical stratification in the GoL. The stratification changes also alter the Mediterranean overturning circulation and the water, heat and salinity exchange with the Atlantic.

Will deep water formation collapse in the North Western Mediterranean Sea by the end of the 21st century?

Iván M. Parras-Berrocal¹, Rubén Vázquez¹, William Cabos², Dimitry V. Sein³, Oscar Álvarez¹, Miguel Bruno¹ and Alfredo Izquierdo¹

¹ Instituto Universitario de Investigación Marina (INMAR), University of Cádiz, Puerto Real, Cádiz, 11510, Spain.

² Departamento de Física y Matemáticas, Universidad de Alcalá, Madrid, 28801, Spain.

³ Alfred Wegener Institute for Polar and Marine Research, Bremerhaven, Germany.

Corresponding author: Iván M. Parras-Berrocal (*ivan.parras@uca.es*)

Key Points:

- The North Western Mediterranean deep water formation collapse by mid-21st century under the RCP8.5 scenario
- The collapse is mostly driven by changes in the properties of the Modified Atlantic Water and Levantine Intermediate Water
- The deep water formation collapse is associated to changes in fluxes through the Strait of Gibraltar

Abstract

Deep water formation (DWF) in the North Western Mediterranean (NWMed) is a key feature of Mediterranean overturning circulation. Changes in DWF under global warming may have an impact on the regional and even on the global climate. Here we analyze the deep convection in the Gulf of Lions (GoL) in a changing climate using an atmosphere-ocean regional coupled model with a high horizontal resolution enough to represent DWF. We find that under the RCP8.5 scenario the NWMed DWF collapses by 2040-2050, leading to almost a 90% shoaling in the winter mixed layer depth by the end of the century. The collapse is mainly related to changes in sea water temperature and salinity of Modified Atlantic Water (MAW) and Levantine Intermediate Water (LIW) that strengthen the vertical stratification in the GoL. The stratification changes also alter the Mediterranean overturning circulation and the water, heat and salinity exchange with the Atlantic.

1 Introduction

The Mediterranean Sea is a semi-enclosed basin where evaporation exceeds precipitation and river run-off causing a deficit in the freshwater balance that is compensated by a net inflow of Atlantic Water (AW) through the Strait of Gibraltar (Bethoux and Gentili, 1999; Millot, 1999; Robinson et al., 2001; Sanchez-Gomez et al., 2011). AW flows through the western and into the eastern basin increasing its density and forming the Modified Atlantic Water (MAW). In winter, the oceanic conditions and the intense local air-sea interactions lead to open-sea intermediate and deep water convection of MAW in the Levantine basin producing the Levantine Intermediate Water (LIW) (Millot, 2014). Then, the LIW spreads westward over intermediate depths (150-600 m) flowing through the Sicily strait and into the Tyrrhenian Sea, reaching the northwestern Mediterranean approximately a decade after its formation (Millot, 2005). The LIW contributes to the Mediterranean outflow from Gibraltar to the Atlantic Ocean, forming the main thermohaline circulation cell of the Mediterranean (Lascaratos et al., 1993; Robinson et al., 2001; Vargas-Yáñez et al., 2012). Winter deep convection also takes place in the Northwestern Mediterranean Sea (NWMed; MEDOC-Group, 1970; Marshall and Schott, 1999; Durrieu de Madron et al., 2013), triggered by the actions of cold and dry regional winds of Mistral (northwesterly) and Tramontane (northerly) (Leaman and Schott, 1991; Somot et al., 2018). The succession of these winds episodes induces intense surface buoyancy loss associated to a rapid surface cooling and strong evaporation (Schott and Leaman, 1991; Seyfried et al., 2017). In the Gulf of Lions (GoL), the regional cyclonic circulation of MAW and of the underlying LIW (warmer and saltier) drives a doming of isopycnals that favors deep convection (Rhein, 1995; Houpert et al., 2016). The doming of isopycnals and the large surface buoyancy loss contribute to the deepening of the convection layer and to the formation of the Western Mediterranean Deep Water (WMDW). The WMDW formation is commonly described in three phases (Marshall and Schott, 1999; Waldman et al., 2017): the preconditioning phase, the intense mixing phase and the restratification-spreading phase.

Besides the main mechanisms commonly associated to deep water formation (DWF), Waldman et al. (2018) point that the intrinsic ocean variability, related to baroclinic instability of the cyclonic gyre, could determine the occurrence or not of deep convection, especially in interannual time scale.

The NWMed DWF, which take place mainly in the GoL and in the Ligurian Sea (Margirier et al., 2020), may be affected by the warmer and dryer conditions expected at the end of the twenty-first century under IPCC scenarios (IPCC 2013; Darmakari et al., 2019; Soto-Navarro et al., 2020). In fact, the Mediterranean Sea is considered a “hot spot” climate change region (Giorgi, 2006), where the mean SST is projected to increase from 0.5°C to 3.1°C (e. g. Somot et al., 2006, 2008; Shaltout and Omstedt, 2014; Adloff et al., 2015; Darmakari et al., 2019; Parras-Berrocal et al., 2020; Soto-Navarro et al., 2020) by the end of the century. The warming may cause an increase in the stratification and thus in the reduction of deep convection (Somot et al., 2006), which is essential in sustaining the Mediterranean overturning circulation.

In the GoL, winter deep convection exhibits a strong interannual variability. The seasonal cycle of the mixed layer depth (MLD) shows very shallow values in summer due to surface warming; while in late winter the MLD presents a clear maximum, eventually deeper than 800-1000 m (D’Ortenzio et al., 2005; Somot et al.,

2018).

The NWMed DWF has been largely studied (MEDOC-Group, 1970; Leaman and Schott, 1991; Durrieu de Madron et al., 2013; Houpert et al., 2016; Margirier et al., 2020) and many attempts to characterize DWF events in the NWMed using high temporal and spatial resolution numerical models have been made (Léger et al., 2016; Seyfried et al., 2017; Waldman et al., 2017; Somot et al., 2018). Most of these works have focused on the impact of atmospheric forcing and ocean preconditioning on the deep convection process. Margirier et al. (2020) found in glider observations that an increase in LIW temperature (0.3°C) and salinity (0.08) limits the winter mixing, blocking the export of heat and salt to deeper layers. An analysis of the yearly maximum MLD in downscaled climate simulations in the framework of the Med-CORDEX project (Soto-Navarro et al., 2020) suggests a strong reduction in the intensity of DWF that is especially noticeable in the GoL, where the averaged maximum MLD of 2043 m will decrease in 1821 m under RCP8.5 by the end of the 21st century. Several studies have analyzed future climate change projections at regional scales (Somot et al., 2006; Shaltout and Omstedt, 2014; Adloff et al., 2015; Darmakari et al., 2019; Parras-Berrocal et al., 2020; Soto-Navarro et al., 2020) but only few of them investigate the DWF response to climate change, pointing to a strong reduction of deep convection (Somot et al., 2006; Adloff et al., 2015; Soto-Navarro et al., 2020). However, the causes of the reduction remain unexplored.

To tackle this issue, a climate change projection under the RCP8.5 scenario is dynamically downscaled with a regionally coupled model. The model appropriately simulates the present time and future climate in the NWMed region (Darmakari et al., 2019; Parras-Berrocal et al., 2020) and is part of the ensemble used in Soto-Navarro et al. (2020), showing the dramatic reduction of DWF intensity reported there. Basing on these premises, the objectives of this work are:

- (i) to quantify the projected reduction of NWMed DWF.
- (ii) to identify the mechanisms leading to that reduction.
- (iii) to assess its impact on the change of the Mediterranean outflow properties into the Atlantic.

The regional coupled system and the experiments used in this work are described in section 2. Section 3 presents the results for the intensity of DWF, the contribution of atmospheric and hydrographic changes and the fluxes through the Strait of Gibraltar. Finally, section 4 contains the discussion and conclusions.

2 Description of Atmosphere Ocean Regional Coupled Model: ROM

We use the atmosphere-ocean regionally coupled model ROM (REMO-OASIS-MPIOM) developed by Sein et al. (2015). ROM comprises the REgional atmosphere MOdel (REMO; Jacob et al., 2001), the Max Planck Institute Ocean Model (MPIOM; Marsland et al., 2003; Jungclaus et al., 2013), the HAMBURG Ocean Carbon Cycle (HAMOCC) model (Maier-Reimer et al., 2005), the Hydrological Discharge (HD) model (Hagemann and Gates, 1998, 2001), a soil model (Rechid and Jacob, 2006) and a dynamic/thermodynamic sea ice model (Hibler, 1979). The atmosphere and the ocean are coupled via OASIS3 (Valcke, 2013) coupler, while the other sub-models are treated as modules either of the atmosphere or the ocean. The model parameterizations and setup used here are described in Parras-Berrocal et al. (2020) who provide a detailed assessment of ROM-simulated present climate and future changes in the Mediterranean.

MPIOM is formulated on an orthogonal curvilinear Arakawa C-grid with a variable horizontal resolution of 7 km (south Alboran Sea) to 25 km (eastern Levantine Sea) in the Mediterranean, with 40 z-levels with increasing layer thickness with depth (Parras-Berrocal et al. 2020).

In this work, we use 1976-2005 as the historical reference period to define the DWF target area in the GoL (Figure 1), and we aim to offer an integrated vision of the impact of climate change on the NWMed DWF under the Representative Concentration Pathway 8.5 (RCP 8.5) for 2006-2099.

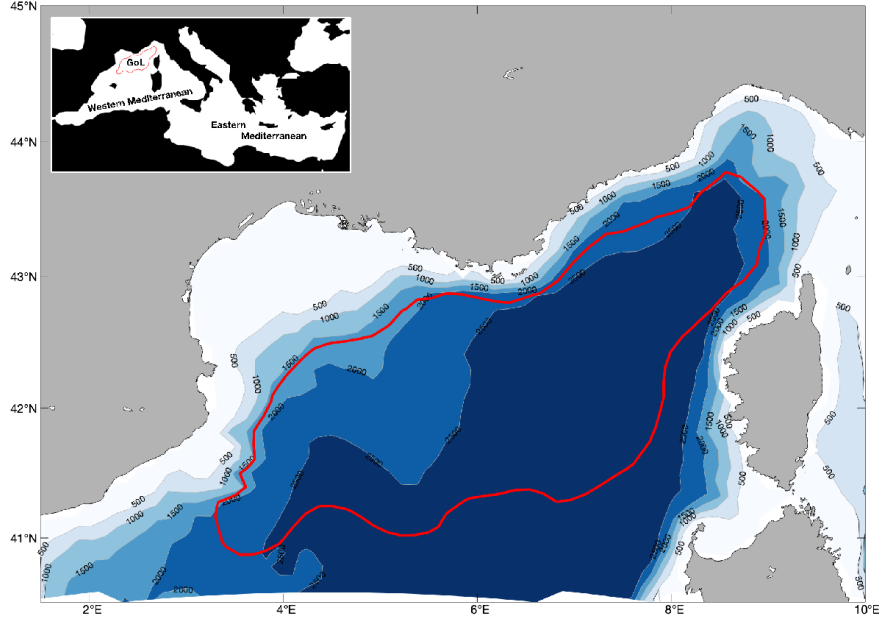


Figure 1. The area representative of the Gulf of Lions DWF used in this study is surrounded by the red line. The ocean model bathymetry (in m) over the NWMed is also shown.

As representative of the GoL we use the mixed patch area surrounded by the red line in Figure 1. Somot et al., (2018) have verified that their results are not very sensitive to the choice of the GoL domain if the continental shelf is avoided and the region where open-sea deep convection occurs is included. The selection of the DWF target area was performed using the mean winter MLD for the 1976–2005 period. The mixed patch area is composed by the grid points where the mean winter MLD is deeper than 1000 m, which corresponds to the depth of WMDW prior to the convection (Waldman et al. 2017).

3 Results

3.1 Intensity of deep water convection in the GoL

The model MLD is defined as the depth, where the density (ρ) has increased by 0.125 kg m^{-3} as compared to the value in the surface box (Wetzel et al., 2004). It is evident a strong reduction of yearly maximum MLD (MLD_{max}) over the GoL by mid-21st century under RCP8.5 emission scenario (Figure 2a). During 2006–2099, the model projects 15 events of deep convection, defined as a MLD_{max} deeper than 1000 m (Herrmann et al., 2010, Somot et al., 2018), with 6 episodes occurring in consecutive years between 2009 and 2014 (see supplementary material: Table S1). These events always correspond to winter months (February–March), when the intense mixing phase is activated.

Our results show a collapse of newly formed WMDW (starting from the 2040–2050 decade no convection is simulated), characterized by MLD_{max} shallower than 500 m (Figure 2a). This result holds independently of the criterion used for MLD definition. Further, we analyze the causes of this collapse.

3.2 Contribution of changes in the winter surface buoyancy loss

The role of the winter air-sea fluxes in the MLD_{max} variability is assessed with the help of the accumulated surface buoyancy loss (BL, eq. 2), defined as the time integral of the buoyancy flux (BF, eq. 1). In turn, the BF is calculated in terms of heat and freshwater fluxes (Marshall and Schott, 1999; Somot et al. 2018):

$$BF = g \cdot \left(\frac{\alpha \cdot Q_{\text{net}}}{\rho_0 \cdot C_p} + \beta \cdot SSS \cdot FWF \right) (1)$$

$$BL(Y) = - \int_{T_1}^{T_2} BF \bullet dt \quad (2)$$

where Q_{net} is the net surface heat flux (positive downward), FWF the net surface freshwater flux (positive downward), g is the gravitational acceleration (9.81 ms^{-2}), α and β the thermal expansion and haline contraction coefficients (respectively calculated as a function of surface T and S), ρ_0 the reference density of sea water 1025 kgm^{-3} , C_p the specific heat capacity of sea water (equal to $4000 \text{ Jkg}^{-1}\text{K}^{-1}$) and SSS the sea surface salinity. Following Somot et al. (2018), the winter accumulated buoyancy loss (BL) (eq. 2) was computed for every year (Y) of the 2006-2099 from December of the previous year (T_1) to March (T_2) and averaged over the GoL.

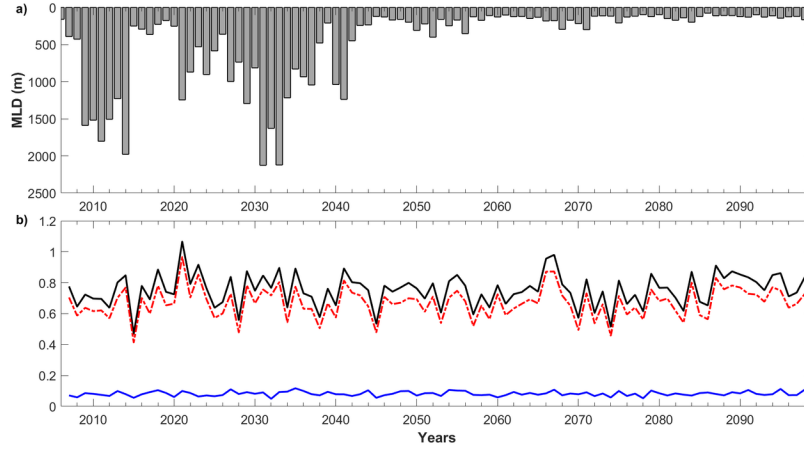


Figure 2. Interannual time series (2006-2099) of RCP8.5 projections of (a) yearly maximum MLD (in m) and (b) integrated buoyancy loss (BL, in m^2s^{-2}) averaged over the GoL. The black line corresponds to the total buoyancy loss, the red dashed line is the heat-related term, and the blue line is the freshwater-related term.

The BL over the GoL along the 2006-2099 period does not show a significant trend and has a mean value of $0.75 \pm 0.12 \text{ m}^2\text{s}^{-2}$. The BL is widely dominated by the heat-related term (mean value of $0.66 \pm 0.12 \text{ m}^2\text{s}^{-2}$). The time series of yearly BL and the heat contribution are well correlated ($r=0.99$) and of the same order of magnitude, while the freshwater term is one order of magnitude smaller and its Pearson correlation coefficient with the BL is 0.61. Our RCP8.5 simulation shows episodes of MLD_{max} deeper than 1000 m only when the BL is above $0.63 \text{ m}^2\text{s}^{-2}$. Although the simulated stronger convective episodes (2014, 2031 and 2033) show a BL ranging from $0.84\text{-}0.90 \text{ m}^2\text{s}^{-2}$, there are years with $MLD_{max} < 200 \text{ m}$ such as 2066, 2067 and 2087, with values of BL $> 0.90 \text{ m}^2\text{s}^{-2}$. This indicates that the BL is not the only factor determining the intensity of the deep water convection and that other factors such as ocean preconditioning could also contribute to the DWF (Margirier et al., 2020).

3.3 Contribution of hydrographic changes in the water column

To analyze the stratification of the water column we have calculated the stratification index (SI); lower values of SI correspond to a less stratified water column. The SI has been previously employed in multiple Mediterranean studies (L'Hévéder et al. 2013, Somot et al. 2018, Margirier et al. 2020) and it is defined as follows (Turner, 1973):

$$SI = \int_0^h N^2 z dz \quad (3)$$

where N is the Brunt-Väisälä frequency ($N^2 = \frac{g}{\rho_0} \frac{\partial \rho}{\partial z}$), z is the depth, ρ the potential density and h the maximum depth of integration which we have chosen to be 1000 m depth.

Under the RCP8.5 scenario, temperature increases through the whole water column (Figure 3a). The detected warming that originally takes place at the surface is transferred progressively to deeper layers (Parras-Berrocal et al., 2020). In the upper layer (0-200 m) the temperature is expected to experience a warming of 2.6°C, while in the intermediate (200-600 m) and 600-1000 m layers will warm by 2.3°C and 0.8°C (Figure 3b), respectively. By the end of 21st century, the MAW flowing in the upper layer of the GoL is projected to slightly freshen (-0.01 psu) while the intermediate (0.4 psu) and 600-1000 m layers (0.2 psu) tend to get saltier (Figure 3c and 3d). The expected increase in temperature and salinity accelerates from 2040 at 200-600 m (Figure 3b and 3d). The 200-600 m depth range corresponds to the equilibrium depth of LIW (Menna and Poulain, 2010) in the western Mediterranean.

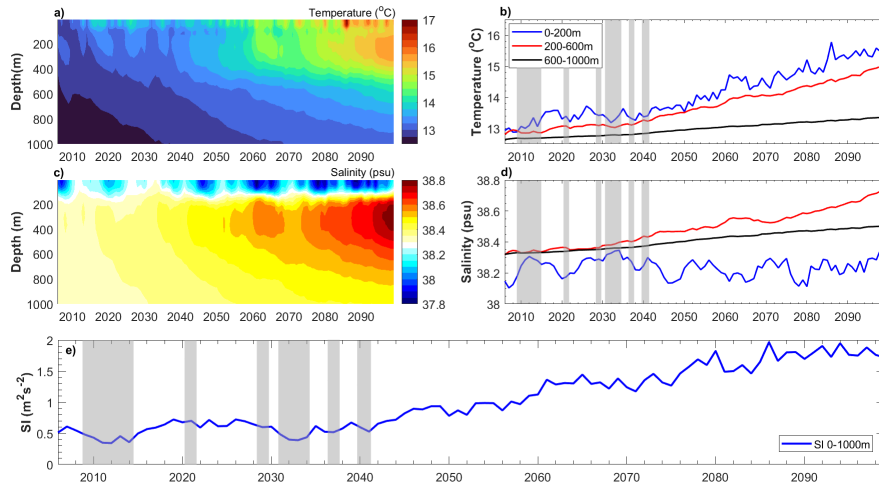


Figure 3 .Interannual time series (2006–2099) of 0–1000 m sea water (a) potential temperature ($^{\circ}\text{C}$) and (c) salinity (psu). The yearly means of (b) potential temperature ($^{\circ}\text{C}$) and (d) salinity (psu) computed for the layers 0–200 m (blue), 200–600 m (red), 600–1000 m (black). (e) The stratification index at 0-1000 m (blue). All time series were simulated by ROM model under the RCP8.5 scenario for winter months (December-January-February-March, DJFM) in the GoL area. The gray bars correspond to DWF episodes ($\text{MLD}_{\text{max}} > 1000$ m depth).

The time evolution of mean winter salinities (Figure 3d) shows a different behavior throughout the water column, showing a slightly freshening trend in MAW and a notable salinization in LIW and the 600-1000 m layer (Table S2).

The yearly SI at 1000 m depth shows values close to minimum values during the projected DWF events (Figure 3e), which suggests a weaker stratification of the water column. Until 2040s the SI does not show any significant trend. However, from 2040 the SI displays an upward trend ($0.02 \text{ m}^2\text{s}^{-2}\text{y}^{-1}$) reaching values up to $1.9 \text{ m}^2\text{s}^{-2}$ at the end of the 21st century. Therefore, the climate change signal introduced by RCP8.5 leads to a higher stratification of the water column which may hamper the formation of deep waters.

3.4 Fluxes at Gibraltar Strait

The simulated water, heat and salt exchange flows through the Strait of Gibraltar are summarized in Table 1. The water outflow in Gibraltar during 2070-2099 (period without DWF episodes) experiences a decrease of 0.04 Sv in comparison with 2006-2041 (period with DWF events), while the net water flow increases by 0.02 Sv. The heat outflux increases $2.6 \cdot 10^{10} \text{ Wyr}^{-1}$ throughout the 2006-2099 period; thus, the Mediterranean Outflow (MO) becomes warmer toward the end of the century: the mean temperature of MO during 2006-2041 is 13.5°C while for the 2070-2099 is 15.2°C . Until 2041 the MO temperature does not present any significant change. However, during the 2041-2099 period the trend of MO temperature displays a sharp increase ($0.034^{\circ}\text{Cyr}^{-1}$, see supplementary: Figure S1).

Table 1. Mean water, heat and salt exchange fluxes, temperature and salinity of inflow and outflow waters at Gibraltar Strait for 2006-2041 and 2070-2099 periods simulated by ROM model under the RCP8.5 scenario. Trends computed from yearly means during 2006-2099. For the net transport calculation, positive values were assigned to inflows and negative to outflows.

	2006-2041	2070-2099	Trend 2006-2099
Water inflow (Sv)	0.544	0.532	$-1.3 \cdot 10^{-4}$ Sv yr ⁻¹
Water outflow (Sv)	0.507	0.476	$-4.2 \cdot 10^{-4}$ Sv yr ⁻¹
Net water flow (Sv)	$3.7 \cdot 10^{-2}$	$5.6 \cdot 10^{-2}$	$3.0 \cdot 10^{-4}$ Sv yr ⁻¹
Heat influx (W)	$3.17 \cdot 10^{13}$	$3.20 \cdot 10^{13}$	$0.7 \cdot 10^{10}$ W yr ⁻¹
Heat outflux (W)	$2.73 \cdot 10^{13}$	$2.88 \cdot 10^{13}$	$2.6 \cdot 10^{10}$ W yr ⁻¹
Net heat transport (W)	$4.4 \cdot 10^{12}$	$3.2 \cdot 10^{12}$	$-1.9 \cdot 10^{10}$ W yr ⁻¹
Salt influx (kg s⁻¹)	$1.68 \cdot 10^7$	$1.65 \cdot 10^7$	$-3.4 \cdot 10^3$ kg s ⁻¹ yr ⁻¹
Salt outflux (kg s⁻¹)	$1.80 \cdot 10^7$	$1.72 \cdot 10^7$	$-1.1 \cdot 10^4$ kg s ⁻¹ yr ⁻¹
Net salt transport (kg s⁻¹)	$-1.2 \cdot 10^6$	$-7.0 \cdot 10^5$	$7.1 \cdot 10^3$ kg s ⁻¹ yr ⁻¹
Temperature of inflow waters (°C)	16.0	16.3	$4.8 \cdot 10^{-3}$ °C yr ⁻¹
Temperature of outflow waters (°C)	13.5	15.2	$2.6 \cdot 10^{-2}$ °C yr ⁻¹
Salinity of inflow waters (psu)	36.3	35.8	$-9.0 \cdot 10^{-3}$ psu yr ⁻¹
Salinity of outflow waters (psu)	38.1	38.2	$2.0 \cdot 10^{-3}$ psu yr ⁻¹

The salinity of the inflow in Gibraltar decreases ($-9.0 \cdot 10^{-3}$ psu yr⁻¹) due to the freshening of the inflowing Atlantic waters. This fresher Atlantic water is the main contributor to the surface freshening in the GoL. Otherwise, the outflow waters become saltier ($+2.0 \cdot 10^{-3}$ psu yr⁻¹) because of the salinization of LIW and deeper waters as shown in Figure 3, thus the salt transport through the Strait to Atlantic Ocean increases (Table 1).

4 Discussion and Conclusions

The response of the NWMed deep water formation to climate change has been explored in Soto-Navarro et al. (2020). The authors found in an ensemble of six Regional Climate Models a robust dramatic decrease of DWF by the end of the 21st century. However, the mechanisms involved were not revealed. As the time evolution of the DWF is strongly model dependent, single model runs can be used to identify in a physically consistent way the causes of this collapse. Therefore, we study these mechanisms in one of the simulations used in Soto-Navarro et al. (2020). Specifically, we analyze the simulation with the regionally coupled system ROM under the RCP8.5 scenario.

Our simulation is able to reproduce the several DWF episodes during the present period: deep convection occurs every year from 2009 to 2014 (Figure 2a and Table S1), what is statistically in good agreement with observations (Houpert et al., 2016; Somot et al., 2018; Margirier et al., 2020).

Starting from the early 2040s, we find a dramatic reduction of MLD_{max} in the GoL (Figure 2a). The maximum MLD for the present climate (1976-2005) is 2385 ± 630 m while for 2070-2099 under the RCP8.5 scenario is 297 ± 47 m. That is, the MLD_{max} simulated by ROM experiences a reduction of almost 90% in the GoL. These values are in close agreement with values reported in Soto-Navarro et al. (2020).

Exploring the possible mechanisms (t. e. air-sea fluxes and ocean preconditioning) that lead to this dramatic MLD_{max} decrease we find that the air-sea fluxes do not seem to be the factor responsible for the DWF collapse, as the buoyancy loss does not change significantly (Figure 2b). Changes in the buoyancy loss also cannot explain the changes in DWF strength, as strong or weak DWF events can happen with similar BL values. In agreement with Somot et al. (2018), our results show that in any case no deep water is formed ($MLD_{max} < 1000$ m) when $BL < 0.6$ m²s⁻² during the 2006-2013 period.

Our results indicate that the changes in properties of the upper and intermediate water masses affecting the

ocean preconditioning are key in the DWF collapse. In our simulation, the temperatures of MAW and LIW are projected to increase 2.6°C and 2.3°C , respectively (Figure 3a and 3b). In turn, the salinity decreases slightly (-0.01 psu) on the surface, while deeper waters become saltier (Figure 3c and 3d). As shown previously in Parras-Berrocal et al. (2020), the warming and freshening signal of MAW comes to the GoL from the Eastern Atlantic, while the increase of LIW temperature and salinity is propagated from its formation area in the Eastern Mediterranean. These changes increase the vertical density gradient between the MAW and LIW, strongly reducing the vertical mixing between these water masses. This is reflected in the stratification index for the 0-1000 m water column (Figure 3e), which from 2040s onward experiences a positive trend ($0.02 \text{ m}^2\text{s}^{-2}\text{y}^{-1}$). Our results do not show a significant change in atmospheric fluxes, changes in MAW and LIW characteristics play the main role in the DWF collapse in the NWMed. The recent study of Margirier et al. (2020) lends some support to our hypothesis: they found in glider and other platforms profiles collected over 2007-2017 that an abrupt jump of LIW temperature and salinity provoked a strong reduction of vertical mixing in the NWMed in 2014. The authors concluded that under those conditions, stronger atmospheric forcing is needed to trigger deep convection. Amitai et al. (2021) have also recently demonstrated that LIW characteristics play a key role in enabling or disabling the deep convection in the GoL. In agreement with Margirier et al. (2020) and Amitai et al. (2021), our results indicate that the projected deep water formation collapse in the 21st century is controlled by the change in LIW characteristics, but we found also that changes in MAW properties play a role. In order to assess the relative contribution of LIW and MAW to the deep water formation collapse we compare the SI calculated from spatially and temporally averaged vertical profiles in the GoL in four cases (Figure S2): (i) using the values corresponding to the pre-collapse period (2006-2041); (ii) using the values corresponding to the post-collapse period (2070-2099); and creating additionally two synthetic profiles, (iii) one containing the pre-collapse characteristics of MAW (0-200 m depth) with the post-collapse properties of deeper layers (200-1000 m depth; Figure S2g), and (iv) a second one with the post-collapse MAW and pre-collapse deeper layers. As seen in Figure S2, there is a clear increase in the post-collapse SI (see also Fig. 3e), but interestingly the SI for the (iv) situation ($1.20 \text{ m}^2\text{s}^{-2}$, Figure S2h) is greater than for the (iii) ($0.97 \text{ m}^2\text{s}^{-2}$, Figure S2g). This results suggest that in the future the change in MAW properties will play a role at least as relevant as LIW in the deep water formation collapse. This collapse of NWMed deep water formation seems to have an impact on the ventilation and on the thermohaline circulation of the Mediterranean Sea.

Both inflow and outflow water transport at the Strait of Gibraltar show a decreasing trend which is larger in the outflow, increasing the net flow (Table 1). Moreover, the incoming surface Atlantic jet will transport more heat and less salt into the Mediterranean basin, causing the hydrographic changes of surface waters (MAW) in the GoL represented in Figure 3. At the same time, the salinization of intermediate (LIW) in the Mediterranean Sea contributes to the increase of MO salinity. As a result, the MO will be warmer and saltier by the end of the 21st century. During the period with DWF episodes (2006-2041) the warming of MO is gradual and does not present noticeable changes, however after the collapse of DWF it accelerates reaching an increase rate of $0.034^{\circ}\text{Cyr}^{-1}$ (Figure S1). Then, the collapse of DWF could be one of the driving factors of the changes in characteristics of fluxes at Gibraltar Strait which reflects changes in the Mediterranean overturning circulation at large scale.

Acknowledgments and Data

I. M. Parras-Berrocal, O. Álvarez and M. Bruno were supported by the Spanish National Research Plan through project TRUCO (RTI2018-100865-BC22). R. Vázquez was supported through a doctoral grant at the University Ferrara and University of Cádiz. W. Cabos have been funded by the Spanish Ministry of Science, Innovation and Universities, the Spanish State Research Agency and the European Regional Development Fund, through grant CGL2017-89583-R. D. Sein was supported in the framework of the state assignment of the Ministry of Science and Higher Education of Russia (0128-2021-0014). The model data are available online (at <https://doi.org/10.5281/zenodo.5151396>).

The authors declare that they have no conflict of interest.

References

Adloff, F., Somot, S., Sevault, F., Jordà, G., Aznar, R., Déqué, M., Herrmann, M., Marcos, M., Dubois, C., Padorno, E., & Alvarez-Fanjul, E. (2015). Mediterranean Sea response to climate change in an ensemble of twenty first century scenarios. *Climate Dynamics*, 45, 2775–2802. <https://doi.org/10.1007/s00382-015-2507-3>

Amitai, Y., Ashkenazy, Y., & Gildor, H. (2021). The Effect of the Source of Deep Water in the Eastern Mediterranean on Western Mediterranean Intermediate and Deep Water. *Frontiers in Marine Science*, 7:615975. <https://doi.org/10.3389/fmars.2020.615975>

Bethoux, J.P., & Gentili, B. (1999). Functioning of the Mediterranean Sea: past and present changes related to freshwater input and climate changes. *Journal of Marine Systems*, 20, 33–47. [https://doi.org/10.1016/S09247963\(98\)00069-4](https://doi.org/10.1016/S09247963(98)00069-4)

Darmaraki, S., Somot, S., Sevault, F., Nabat, P., Cabos Narvaez, W. D., Cavicchia, L., Djurdjevic, V., Li, L., Sannino, G., & Sein, D. V. (2019). Future evolution of Marine Heatwaves in the Mediterranean Sea, *Climate Dynamics*, 53, 1371–1392. <https://doi.org/10.1007/s00382-019-04661-z>

D’Ortenzio, F., Iudicone, D., de Boyer Montegut, C., Testor, P., Antoine, D., Marullo, S., Santoreli, R., & Madec, G. (2005). Seasonal variability of the mixed layer depth in the mediterranean sea as derived from in situ profiles. *Geophysical Research Letter*, 32, L12605. <https://doi.org/10.1029/2005GL022463>

Durrieu de Madron, X., Houpert, L., Puig, P., Sanchez-Vidal, A., Testor, P., Bosse, A., Estournel, C., Somot, S., Bourrin, F., Bouin, M. N., Beauverger, M., Beguery, L., Calafat, A., Canals, M., Cassou, C., Coppola, L., Dausse, D., D’Ortenzio, F., Font, J., Heussner, S., Kunesch, S., Lefevre, D., Goff, H. L., Martin, J., Mortier, L., Palanques, A., & Raimbault, P. (2013). Interaction of dense shelf water cascading and open-sea convection in the Northwestern Mediterranean during winter 2012. *Geophysical Research Letter*, 40, 1379–1385. <https://doi.org/10.1002/grl.50331>

Giorgetta, M. A., Jungclaus, J., Reick, C. H., Legutke, S., Bader, J., Böttinger, M., Brovkin, V., Crueger, T., Esch, M., Fieg, K., Glushak, K., Gayler, V., Haak, H., Hollweg, H.-D., Ilyina, T., Kinne, S., Kornbluh, L., Matei, D., Mauritsen, T., Mikolajewicz, U., Mueller, W., Notz, D., Pithan, F., Raddatz, T., Rast, S., Redler, R., Roeckner, E., Schmidt, H., Schnur, R., Segschneider, J., Six, K. D., Stockhause, M., Timmreck, C., Wegner, J., Widmann, H., Wieners, K.-H., Claussen, M., Marotzke, J., & Stevens, B. (2013). Climate and carbon cycle changes from 1850 to 2100 in MPI-ESM simulations for the Coupled Model Intercomparison Project phase 5. *Journal of Advances in Modelling Earth Systems*, 5, 572–597, <https://doi.org/10.1002/jame.20038>

Giorgi, F. (2006). Climate change hot-spots. *Geophysical Research Letter*, 33, L08707. <https://doi.org/10.1029/2006GL025734>

Hagemann, S., & Dümenil-Gates, L. (1998). A parameterization of the lateral waterflow for the global scale *Climate Dynamics*, 14, 17–31. <https://doi.org/10.1007/s003820050205>

Hagemann, S. & Dümenil-Gates, L. (2001). Validation of the hydrological cycle of ECMWF and NCEP reanalysis using the MPI hydrological discharge model. *Journal Geophysical Research*, 106, 1503–1510. <https://doi.org/10.1029/2000JD900568>

Herrmann, M., Sevault, F., Beuvier, J., & Somot, S. (2010). What induced the exceptional 2005 convection event in the northwestern Mediterranean basin? Answers from a modeling study. *Journal Geophysical Research: Oceans*, 115(C12)051. <https://doi.org/10.1029/2010JC006162>

Hibler, W. D. (1979). A dynamic thermodynamic sea ice model. *Journal of Physical Oceanography*, 9, 815–846. [https://doi.org/10.1175/1520-0485\(1979\)009<0815:ADTSIM>2.0.CO;2](https://doi.org/10.1175/1520-0485(1979)009<0815:ADTSIM>2.0.CO;2)

Houpert, L., Durrieu de Madron, X., Testor, P., Bosse, A., D’Ortenzio, F., Bouin, M. N., Dausse, D., Le Goff, H., Kunesch, S., Labaste, M., & Coppola, L. (2016). Observations of open-ocean deep convection in the northwestern Mediterranean Sea: Seasonal and interannual variability of mixing and deep

water masses for the 2007-2013 period. *Journal of Geophysical Research: Oceans*, 121(11), 8139-8171. <https://doi.org/10.1002/2016JC011857>

IPCC. (2013). *Climate Change 2013: The Physical Science Basis. Contribution of Working Group I to the Fifth Assessment Report of the Intergovernmental Panel on Climate Change* (Stocker TF, Qin D, Plattner G-K, Tignor M, Allen SK, Boschung J, Nauels A, Xia Y, Bex V and Midgley PM (eds)). Cambridge University Press, Cambridge and New York, pp 1535

Jacob, D. (2001). A note to the simulation of the annual and interannual variability of the water budget over the Baltic Sea drainage basin. *Meteorology and Atmospheric Physics*, 77, 61–73. <https://doi.org/10.1007/s007030170017>

Jungclauss, J. H., Fischer, N., Haak, H., Lohmann, K., Marotzke, J., Matei, D., Mikolajewicz, U., Notz, D., & von Storch, J. S. (2013). Characteristics of the ocean simulations in MPIOM, the ocean component of the MPI-Earth system model. *Journal of Advances in Modelling Earth Systems*, 5, 422–446. <https://doi.org/10.1002/jame.20023>

Lasarcatos, A., Williams, R., & Tragou, E. (1993). A mixed-layer study of the formation of Levantine Intermediate Water. *Journal Geophysical Research*, 98(C8), 14739–14749. <https://doi.org/10.1029/93JC00912>

Leaman, K., & Schott, F. (1991). Hydrographic structure of the convection regime in the Gulf of Lions: Winter 1987. *Journal of Physical Oceanography*, 21(4), 575–598.

Leger, F., Lebeaupin Brossier, C., Giordani, H., Arsouze, T., Beuvier, J., Bouin, M.-N., Bresson, E., Ducrocq, V., Fourrie, N., & Nuret, M. (2016). Dense water formation in the north-western Mediterranean area during HyMeX-SOP2 in 1/36° ocean simulations: Sensitivity to initial conditions. *Journal Geophysical Research: Oceans*, 121(8), 5549–5569. <https://doi.org/10.1002/2015JC011542>

L'Hévéder, B. Li, L. Sevault, F. & Somot, S. (2013). Interannual variability of deep convection in the Northwestern Mediterranean simulated with a coupled AORCM. *Climate Dynamics*, 41(3–4), 937–960. <https://doi.org/10.1007/s00382-012-1527-5>

Maier-Reimer, E., Kriest, I., Segsneider, J., & Wetzel, P. (2005). The HAMburg Ocean Carbon Cycle Model HAMOCC5.1 Technical Description Release 1.1, Ber. Erdsystemforschung, 14, available at: <http://hdl.handle.net/11858/00-001M-0000-0011-FF5C-D>

Margirier, F., Testor, P., Heslop, E., Mallil, K., Bosse, A., Houpert, L., Mortier, L., Bouin, M.-B., Coppola, L., D'Ortenzio, F., Durrie de Madron, X., Mourre, B., Prieur, L., Raimbault, P. & Taillandier, V. (2020). Abrupt warming and salinification of intermediate waters interplays with decline of deep convection in the Northwestern Mediterranean Sea. *Scientific Reports* 10, 20923. <https://doi.org/10.1038/s41598-020-77859-5>

Marshall, J., & Schott, F. (1999). Open-ocean convection: observations, theory, and models. *Reviews of Geophysics*, 37(1), 1–64. <https://doi.org/10.1029/98RG02739>

Marsland, S. J., Haak, H., Jungclauss, J. H., Latif, M., & Roeske, F. (2003). The Max-Planck- Institute global ocean/sea ice model with orthogonal curvilinear coordinates. *Ocean Modelling*, 5 (2), 91–127, [https://doi.org/10.1016/S1463-5003\(02\)00015-X](https://doi.org/10.1016/S1463-5003(02)00015-X)

MEDOC Group. (1970). Observations of formation of deep-water in the Mediterranean Sea. *Nature*, 227, 1037–1040. <https://doi.org/10.1038/2271037a0>

Menna, M. & Poulain, P. M. (2010). Mediterranean intermediate circulation estimated from Argo data in 2003–2010. *Ocean Science*, 6, 331–343. <https://doi.org/10.5194/os-6-331-2010>

Mertens, C., & Schott, F. (1998). Interannual variability of deep-water formation in the northwestern Mediterranean. *Journal of Physical Oceanography*, 28, 1410–1423, [https://doi.org/10.1175/1520-0485\(1998\)028<1410:IVODWF>2.0.CO;2](https://doi.org/10.1175/1520-0485(1998)028<1410:IVODWF>2.0.CO;2)

- Mikolajewicz, U., Sein, D. V., Jacob, D., Königk, T., Podzun, R. & Semmler, T. (2005). Simulating Arctic sea ice variability with a coupled regional atmosphere-ocean-sea ice model. *Meteorologische Zeitschrift*, 14 (6), 793–800. <https://doi.org/10.1127/0941-2948/2005/0083>
- Millot, C. (1999). Circulation in the Western Mediterranean Sea, *Journal of Marine Systems*, 20 (1-4), 423-440. [https://doi.org/10.1016/S0924-7963\(98\)00078-5](https://doi.org/10.1016/S0924-7963(98)00078-5)
- Millot, C. (2005). Circulation in the mediterranean sea: Evidences, debates and unanswered questions, *Scientia Marina*, 69, 5–21. <https://doi.org/10.3989/scimar.2005.69s15>
- Millot, C. (2014). Levantine Intermediate Water characteristics: an astounding general misunderstanding! (addendum), *Scientia Marina*, 78(2), 165–171. <https://doi.org/10.3989/scimar.04045.30H>
- Parras-Berrocal, I. M., Vazquez, R., Cabos, W., Sein, D., Mañanes, R., Perez-Sanz, J., & Izquierdo, A. (2020). The climate change signal in the Mediterranean Sea in a regionally coupled atmosphere–ocean model, *Ocean Science*, 16, 743–765. <https://doi.org/10.5194/os-16-743-2020>
- Rechid, D., & Jacob, D.: Influence of monthly varying vegetation on the simulated climate in Europe. *Meteorologische Zeitschrift*, 15(1), 99–116. <https://doi.org/10.1127/0941-2948/2006/0091>
- Rhein, M. (1995). Deep water formation in western Mediterranean. *Journal of Geophysical Research*, 100-C4, 6943-6959. <https://doi.org/10.1029/94JC03198>
- Robinson, A., Leslie, W., Theocharis, A., & Lascaratos, A. (2001). *Encyclopedia of ocean sciences*. Academic Press Ltd., London chap Mediterranean Sea Circulation
- Sánchez-Gómez, E., Somot, S., Josey, S. A., Dubois, C., Elguindi, N., & Déqué, M. (2011). Evaluation of Mediterranean Sea water and heat budgets simulated by an ensemble of high resolution regional climate models. *Climate Dynamics*, 37, 2067–2086. <https://doi.org/10.1007/s00382-011-1012-6>
- Schott, F., & Leaman, K. D. (1991). Observations with Moored Acoustic Doppler Current Profilers in the Convection Regime in the Golfe du Lion. *Journal of Physical Oceanography*, 21, 558–574, [https://doi.org/10.1175/1520-0485\(1991\)021<0558:OWMADC>2.0.CO;2](https://doi.org/10.1175/1520-0485(1991)021<0558:OWMADC>2.0.CO;2)
- Sein, D. V., Mikolajewicz, U., Gröger, M., Fast, I., Cabos, W., Pinto, J. G., Hagemann, S., Semmler, T., Izquierdo, A., & Jacob, D. (2015). Regionally coupled atmosphere-ocean- sea ice-marine biogeochemistry model ROM: 1. Description and validation, *Journal of Advance in Modelling Earth Systems*, 7(1), 268–304. <https://doi.org/10.1002/2014MS000357>
- Sein, D. V., Gröger, M., Cabos, W., Alvarez-Garcia, F. J., Hagemann, S., Pinto, J. G., Izquierdo, A., de la Vara, A., Koldunov, N. V., Dvornikov, A. Y., Limareva, N., Alekseeva, E., Martinez-Lopez, B. & Jacob, D. (2020). Regionally coupled atmosphere-ocean- sea ice-marine biogeochemistry model ROM: 2. Studying the Climate Change Signal in the North Atlantic and Europe, *Journal of Advance in Modelling Earth Systems*, 12, e2019MS001646. <https://doi.org/10.1029/2019Ms001646>
- Seyfried, L., Marsaleix, P., Richard, E., & Estournel, C. (2017). Modelling deep-water formation in the north-west Mediterranean Sea with a new air–sea coupled model: sensitivity to turbulent flux parameterizations. *Ocean Science*, 13, 1093–1112. <https://doi.org/10.5194/os-13-1093-2017>
- Shaltout, M., & Omstedt, A. (2014). Recent sea surface temperature trends and future scenarios for the Mediterranean Sea. *Oceanologia*, 56, 411–443. <https://doi.org/10.5697/oc.56-3.411>
- Somot, S., Sevault, F., & Déqué, M. (2006). Transient climate change scenario simulation of the Mediterranean Sea for the 21st century using a high-resolution ocean circulation model. *Climate Dynamics*, 27, 851–879. <https://doi.org/10.1007/s00382-006-0167-z>
- Somot, S., Sevault, F., Déqué, M., & Crépon, M. (2008). 21st century climate change scenario for the Mediterranean using a coupled atmosphere–ocean regional climate model. *Global Planetary Change*, 63, 112–126. <https://doi.org/10.1016/j.gloplacha.2007.10.003>

- Somot, S., Houpert, L., Sevault, F., Testor, P., Bosse, A., Taupier-Letage, I., Bouin, M. N., Waldman, R., Cassou, C., Sanchez-Gomez, E., Durrieu de Madron, X., Adloff, F., Nabat, P. & Herrman, M. (2018). Characterizing, modelling and understanding the climate variability of the deep water formation in the North-Western Mediterranean Sea. *Climate Dynamics*, 51, 1179–1210. <https://doi.org/10.1007/s00382-016-3295-0>
- Soto-Navarro, J., Jordá, G., Amores, A., Cabos, W., Somot, S., Sevault, F., Macias, D., Djurdjevic, V., Sanino, G., Li, L. & Sein, D. (2020). Evolution of Mediterranean Sea water properties under climate change scenarios in the Med-CORDEX ensemble. *Climate Dynamics*, 54, 2135–2165. <https://doi.org/10.1007/s00382-019-05105-4>
- Taylor, K., Stouffer, R., & Meehl, G. (2012). An overview of CMIP5 and the experiments design. *Bulletin of the American Meteorological Society*, 93, 485–498. <https://doi.org/10.1175/BAMS-D-11-00094.1>
- Valcke, S. (2013). The OASIS3 coupler: a European climate modelling community software. *Geoscientific Model Development*, 6, 373–388. <https://doi.org/10.5194/gmd-6-373-2013>
- Turner, J. (1973). *Buoyancy effects in fluids: Cambridge monographs on mechanics and applied mathematics*. Cambridge University Press, Cambridge
- Vargas-Yáñez, M., Zunino, P., Schroeder, K., López-Jurado, J. L., Plaza, F., Serra, M., Castro, C., García-Martínez, M. C., Moya, F. & Salat, J. (2012). Extreme Western Intermediate Water formation in winter 2010. *Journal of Marine Systems*, 105-10, 52-59. <https://doi.org/10.1016/j.jmarsys.2012.05.010>
- Waldman, R., Somot, S., Herrmann, M., Bosse, A., Caniaux, G., Estournel, C., Houpert, L., Prieur, L., Sevault, F., & Testor, P. (2017). Modelling the intense 2012–2013 dense water formation event in the northwestern Mediterranean Sea: Evaluation with an ensemble a simulation approach. *Journal of Geophysical Research: Oceans*, 122, 1297–1324. <https://doi.org/10.1002/2016JC012437>
- Waldman, R., Somot, S., Herrmann, M., Sevault, F., & Isachsen, P. E. (2018). On the Chaotic Variability of Deep Convection in the Mediterranean Sea. *Geophysical Research Letters*, 45,2433-2443. <https://doi.org/10.1002/2017GL076319>
- Wetzel, P., Haak, H., Jungclauss, J., & Maier-Reimer, E. (2004). The Max-Planck-institute global ocean/sea ice model. Model MPI-OM Technical report. http://www.mpimet.mpg.de/fileadmin/models/MPIOM/DRAFT_MPIOM_TECHNICAL_REPORT.pdf

Will deep water formation collapse in the North Western Mediterranean Sea by the end of the 21st century?

Iván M. Parras-Berrocal¹, Rubén Vázquez¹, William Cabos², Dmitry V. Sein³, Oscar Álvarez¹, Miguel Bruno¹ and Alfredo Izquierdo¹

¹ Instituto Universitario de Investigación Marina (INMAR), University of Cádiz, Puerto Real, Cádiz, 11510, Spain.

² Departamento de Física y Matemáticas, Universidad de Alcalá, Madrid, 28801, Spain.

³ Alfred Wegener Institute for Polar and Marine Research, Bremerhaven, Germany.

Corresponding author: Iván M. Parras-Berrocal (ivan.parras@uca.es)

Key Points:

- The North Western Mediterranean deep water formation collapse by mid-21st century under the RCP8.5 scenario
- The collapse is mostly driven by changes in the properties of the Modified Atlantic Water and Levantine Intermediate Water
- The deep water formation collapse is associated to changes in fluxes through the Strait of Gibraltar

Abstract

Deep water formation (DWF) in the North Western Mediterranean (NWMed) is a key feature of Mediterranean overturning circulation. Changes in DWF under global warming may have an impact on the regional and even on the global climate. Here we analyze the deep convection in the Gulf of Lions (GoL) in a changing climate using an atmosphere-ocean regional coupled model with a high horizontal resolution enough to represent DWF. We find that under the RCP8.5 scenario the NWMed DWF collapses by 2040-2050, leading to almost a 90% shoaling in the winter mixed layer depth by the end of the century. The collapse is mainly related to changes in sea water temperature and salinity of Modified Atlantic Water (MAW) and Levantine Intermediate Water (LIW) that strengthen the vertical stratification in the GoL. The stratification changes also alter the Mediterranean overturning circulation and the water, heat and salinity exchange with the Atlantic.

1 Introduction

The Mediterranean Sea is a semi-enclosed basin where evaporation exceeds precipitation and river run-off causing a deficit in the freshwater balance that is compensated by a net inflow of Atlantic Water (AW) through the Strait of Gibraltar (Bethoux and Gentili, 1999; Millot, 1999; Robinson et al., 2001; Sanchez-Gomez et al., 2011). AW flows through the western and into the eastern basin increasing its density and forming the Modified Atlantic Water (MAW). In winter, the

oceanic conditions and the intense local air–sea interactions lead to open–sea intermediate and deep water convection of MAW in the Levantine basin producing the Levantine Intermediate Water (LIW) (Millot, 2014). Then, the LIW spreads westward over intermediate depths (150–600 m) flowing through the Sicily strait and into the Tyrrhenian Sea, reaching the northwestern Mediterranean approximately a decade after its formation (Millot, 2005). The LIW contributes to the Mediterranean outflow from Gibraltar to the Atlantic Ocean, forming the main thermohaline circulation cell of the Mediterranean (Lascaratos et al., 1993; Robinson et al., 2001; Vargas-Yáñez et al., 2012). Winter deep convection also takes place in the Northwestern Mediterranean Sea (NWMed; MEDOC-Group, 1970; Marshall and Schott, 1999; Durrieu de Madron et al., 2013), triggered by the actions of cold and dry regional winds of Mistral (northwesterly) and Tramontane (northerly) (Leaman and Schott, 1991; Somot et al., 2018). The succession of these winds episodes induces intense surface buoyancy loss associated to a rapid surface cooling and strong evaporation (Schott and Leaman, 1991; Seyfried et al., 2017). In the Gulf of Lions (GoL), the regional cyclonic circulation of MAW and of the underlying LIW (warmer and saltier) drives a doming of isopycnals that favors deep convection (Rhein, 1995; Houpert et al., 2016). The doming of isopycnals and the large surface buoyancy loss contribute to the deepening of the convection layer and to the formation of the Western Mediterranean Deep Water (WMDW). The WMDW formation is commonly described in three phases (Marshall and Schott, 1999; Waldman et al., 2017): the preconditioning phase, the intense mixing phase and the restratification-spreading phase.

Besides the main mechanisms commonly associated to deep water formation (DWF), Waldman et al. (2018) point that the intrinsic ocean variability, related to baroclinic instability of the cyclonic gyre, could determinate the occurrence or not of deep convection, especially in interannual time scale.

The NWMed DWF, which take place mainly in the GoL and in the Ligurian Sea (Margirier et al., 2020), may be affected by the warmer and dryer conditions expected at the end of the twenty-first century under IPCC scenarios (IPCC 2013; Darmakari et al., 2019; Soto-Navarro et al., 2020). In fact, the Mediterranean Sea is considered a “hot spot” climate change region (Giorgi, 2006), where the mean SST is projected to increase from 0.5°C to 3.1°C (e. g. Somot et al., 2006, 2008; Shaltout and Omstedt, 2014; Adloff et al., 2015; Darmakari et al., 2019; Parras-Berrocal et al., 2020; Soto-Navarro et al., 2020) by the end of the century. The warming may cause an increase in the stratification and thus in the reduction of deep convection (Somot et al., 2006), which is essential in sustaining the Mediterranean overturning circulation.

In the GoL, winter deep convection exhibits a strong interannual variability. The seasonal cycle of the mixed layer depth (MLD) shows very shallow values in summer due to surface warming; while in late winter the MLD presents a clear maximum, eventually deeper than 800–1000 m (D’Ortenzio et al., 2005; Somot et al., 2018).

The NWMed DWF has been largely studied (MEDOC-Group, 1970; Leaman and Schott, 1991; Durrieu de Madron et al., 2013; Houpert et al., 2016; Margirier et al., 2020) and many attempts to characterize DWF events in the NWMed using high temporal and spatial resolution numerical models have been made (Léger et al., 2016; Seyfried et al., 2017; Waldman et al., 2017; Somot et al., 2018). Most of these works have focused on the impact of atmospheric forcing and ocean preconditioning on the deep convection process. Margirier et al. (2020) found in glider observations that an increase in LIW temperature (0.3°C) and salinity (0.08) limits the winter mixing, blocking the export of heat and salt to deeper layers. An analysis of the yearly maximum MLD in downscaled climate simulations in the framework of the Med-CORDEX project (Soto-Navarro et al., 2020) suggests a strong reduction in the intensity of DWF that is especially noticeable in the GoL, where the averaged maximum MLD of 2043 m will decrease in 1821 m under RCP8.5 by the end of the 21st century. Several studies have analyzed future climate change projections at regional scales (Somot et al., 2006; Shaltout and Omstedt, 2014; Adloff et al., 2015; Darmakari et al., 2019; Parras-Berrocal et al., 2020; Soto-Navarro et al., 2020) but only few of them investigate the DWF response to climate change, pointing to a strong reduction of deep convection (Somot et al., 2006; Adloff et al., 2015; Soto-Navarro et al., 2020). However, the causes of the reduction remain unexplored.

To tackle this issue, a climate change projection under the RCP8.5 scenario is dynamically downscaled with a regionally coupled model. The model appropriately simulates the present time and future climate in the NWMed region (Darmakari et al., 2019; Parras-Berrocal et al., 2020) and is part of the ensemble used in Soto-Navarro et al. (2020), showing the dramatic reduction of DWF intensity reported there. Basing on these premises, the objectives of this work are:

- (i) to quantify the projected reduction of NWMed DWF.
- (ii) to identify the mechanisms leading to that reduction.
- (iii) to assess its impact on the change of the Mediterranean outflow properties into the Atlantic.

The regional coupled system and the experiments used in this work are described in section 2. Section 3 presents the results for the intensity of DWF, the contribution of atmospheric and hydrographic changes and the fluxes through the Strait of Gibraltar. Finally, section 4 contains the discussion and conclusions.

2 Description of Atmosphere Ocean Regional Coupled Model: ROM

We use the atmosphere-ocean regionally coupled model ROM (REMO-OASIS-MPIOM) developed by Sein et al. (2015). ROM comprises the REgional atmosphere MOdel (REMO; Jacob et al., 2001), the Max Planck Institute Ocean Model (MPIOM; Marsland et al., 2003; Jungclaus et al., 2013), the HAMburg Ocean Carbon Cycle (HAMOCC) model (Maier-Reimer et al., 2005), the Hydrological Discharge (HD) model (Hagemann and Gates, 1998, 2001), a soil

model (Rechid and Jacob, 2006) and a dynamic/thermodynamic sea ice model (Hibler, 1979). The atmosphere and the ocean are coupled via OASIS3 (Valcke, 2013) coupler, while the other sub-models are treated as modules either of the atmosphere or the ocean. The model parameterizations and setup used here are described in Parras-Berrocal et al. (2020) who provide a detailed assessment of ROM-simulated present climate and future changes in the Mediterranean.

MPIOM is formulated on an orthogonal curvilinear Arakawa C-grid with a variable horizontal resolution of 7 km (south Alboran Sea) to 25 km (eastern Levantine Sea) in the Mediterranean, with 40 z-levels with increasing layer thickness with depth (Parras-Berrocal et al. 2020).

In this work, we use 1976-2005 as the historical reference period to define the DWF target area in the GoL (Figure 1), and we aim to offer an integrated vision of the impact of climate change on the NWMed DWF under the Representative Concentration Pathway 8.5 (RCP 8.5) for 2006-2099.

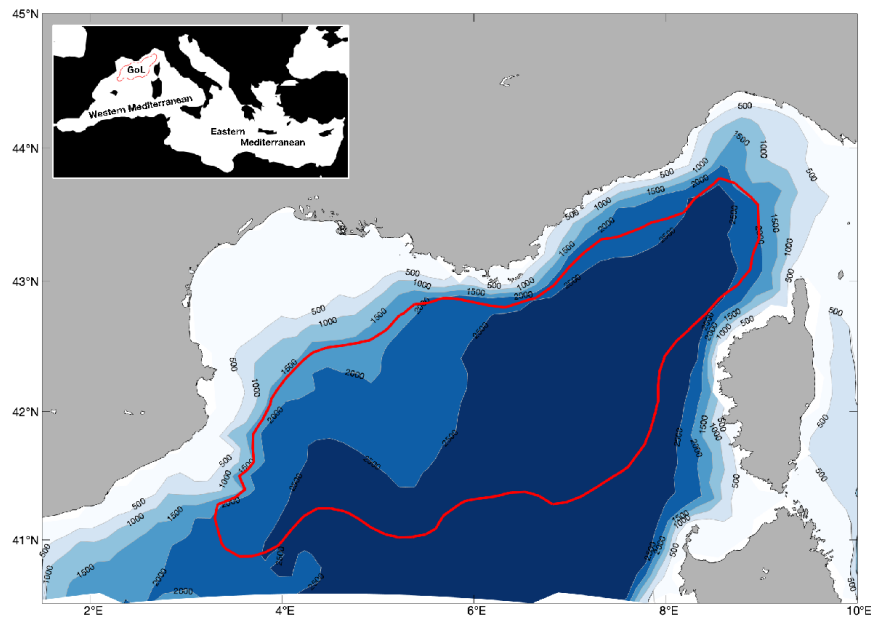


Figure 1. The area representative of the Gulf of Lions DWF used in this study is surrounded by the red line. The ocean model bathymetry (in m) over the NWMed is also shown.

As representative of the GoL we use the mixed patch area surrounded by the red line in Figure 1. Somot et al., (2018) have verified that their results are not very sensitive to the choice of the GoL domain if the continental shelf is avoided and the region where open-sea deep convection occurs is included. The selection of the DWF target area was performed using the mean winter MLD for the 1976–2005 period. The mixed patch area is composed by the grid points where the mean winter MLD is deeper than 1000 m, which corresponds to the

depth of WMDW prior to the convection (Waldman et al. 2017).

3 Results

3.1 Intensity of deep water convection in the GoL

The model MLD is defined as the depth, where the density (ρ) has increased by 0.125 kg m^{-3} as compared to the value in the surface box (Wetzel et al., 2004). It is evident a strong reduction of yearly maximum MLD (MLD_{max}) over the GoL by mid-21st century under RCP8.5 emission scenario (Figure 2a). During 2006-2099, the model projects 15 events of deep convection, defined as a MLD_{max} deeper than 1000 m (Herrmann et al., 2010, Somot et al., 2018), with 6 episodes occurring in consecutive years between 2009 and 2014 (see supplementary material: Table S1). These events always correspond to winter months (February-March), when the intense mixing phase is activated.

Our results show a collapse of newly formed WMDW (starting from the 2040–2050 decade no convection is simulated), characterized by MLD_{max} shallower than 500 m (Figure 2a). This result holds independently of the criterion used for MLD definition. Further, we analyze the causes of this collapse.

3.2 Contribution of changes in the winter surface buoyancy loss

The role of the winter air-sea fluxes in the MLD_{max} variability is assessed with the help of the accumulated surface buoyancy loss (BL, eq. 2), defined as the time integral of the buoyancy flux (BF, eq. 1). In turn, the BF is calculated in terms of heat and freshwater fluxes (Marshall and Schott, 1999; Somot et al. 2018):

$$BF = g \bullet \left(\frac{\alpha \bullet Q_{net}}{\rho_0 \bullet C_p} + \beta \bullet SSS \bullet FWF \right) \quad (1)$$

$$BL(Y) = - \int_{T_1}^{T_2} BF \bullet dt \quad (2)$$

where Q_{net} is the net surface heat flux (positive downward), FWF the net surface freshwater flux (positive downward), g is the gravitational acceleration (9.81 ms^{-2}), and α and β the thermal expansion and haline contraction coefficients (respectively calculated as a function of surface T and S), ρ_0 the reference density of sea water 1025 kgm^{-3} , C_p the specific heat capacity of sea water (equal to $4000 \text{ Jkg}^{-1}\text{K}^{-1}$) and SSS the sea surface salinity. Following Somot et al. (2018), the winter accumulated buoyancy loss (BL) (eq. 2) was computed for every year (Y) of the 2006-2099 from December of the previous year (T_1) to March (T_2) and averaged over the GoL.

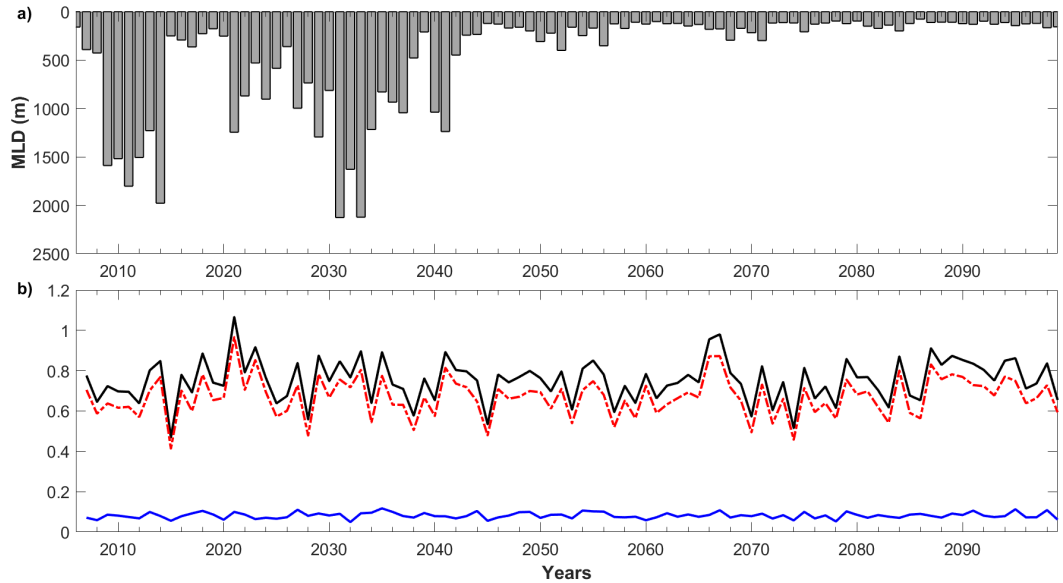


Figure 2. Interannual time series (2006-2099) of RCP8.5 projections of (a) yearly maximum MLD (in m) and (b) integrated buoyancy loss (BL, in m^2s^{-2}) averaged over the GoL. The black line corresponds to the total buoyancy loss, the red dashed line is the heat-related term, and the blue line is the freshwater-related term.

The BL over the GoL along the 2006-2099 period does not show a significant trend and has a mean value of $0.75 \pm 0.12 \text{ m}^2\text{s}^{-2}$. The BL is widely dominated by the heat-related term (mean value of $0.66 \pm 0.12 \text{ m}^2\text{s}^{-2}$). The time series of yearly BL and the heat contribution are well correlated ($r=0.99$) and of the same order of magnitude, while the freshwater term is one order of magnitude smaller and its Pearson correlation coefficient with the BL is 0.61. Our RCP8.5 simulation shows episodes of MLD_{max} deeper than 1000 m only when the BL is above $0.63 \text{ m}^2\text{s}^{-2}$. Although the simulated stronger convective episodes (2014, 2031 and 2033) show a BL ranging from $0.84\text{-}0.90 \text{ m}^2\text{s}^{-2}$, there are years with $\text{MLD}_{\text{max}} < 200 \text{ m}$ such as 2066, 2067 and 2087, with values of BL $> 0.90 \text{ m}^2\text{s}^{-2}$. This indicates that the BL is not the only factor determining the intensity of the deep water convection and that other factors such as ocean preconditioning could also contribute to the DWF (Margirier et al., 2020).

3.3 Contribution of hydrographic changes in the water column

To analyze the stratification of the water column we have calculated the stratification index (SI); lower values of SI correspond to a less stratified water column. The SI has been previously employed in multiple Mediterranean studies (L'Hévéder et al. 2013, Somot et al. 2018, Margirier et al. 2020) and it is defined as follows (Turner, 1973):

$$SI = \int_0^h N^2 z dz \quad (3)$$

where N is the Brunt-Väisälä frequency ($N^2 = \frac{g}{\rho_0} \frac{\partial \rho}{\partial z}$), z is the depth, ρ the potential density and h the maximum depth of integration which we have chosen to be 1000 m depth.

Under the RCP8.5 scenario, temperature increases through the whole water column (Figure 3a). The detected warming that originally takes place at the surface is transferred progressively to deeper layers (Parras-Berrocal et al., 2020). In the upper layer (0-200 m) the temperature is expected to experience a warming of 2.6°C, while in the intermediate (200-600 m) and 600-1000 m layers will warm by 2.3°C and 0.8°C (Figure 3b), respectively. By the end of 21st century, the MAW flowing in the upper layer of the GoL is projected to slightly freshen (-0.01 psu) while the intermediate (0.4 psu) and 600-1000 m layers (0.2 psu) tend to get saltier (Figure 3c and 3d). The expected increase in temperature and salinity accelerates from 2040 at 200-600 m (Figure 3b and 3d). The 200-600 m depth range corresponds to the equilibrium depth of LIW (Menna and Poulain, 2010) in the western Mediterranean.

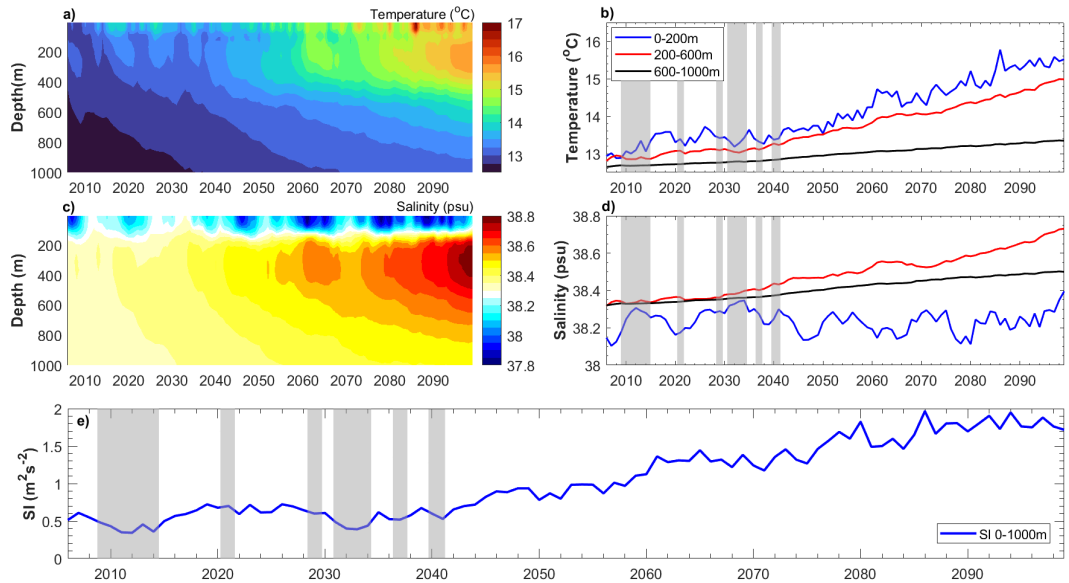


Figure 3. Interannual time series (2006–2099) of 0–1000 m sea water (a) potential temperature (°C) and (c) salinity (psu). The yearly means of (b) potential temperature (°C) and (d) salinity (psu) computed for the layers 0–200 m (blue), 200–600 m (red), 600–1000 m (black). (e) The stratification index at 0-1000 m (blue). All time series were simulated by ROM model under the RCP8.5 scenario for winter months (December-January-February-March, DJFM) in the GoL area. The gray bars correspond to DWF episodes ($MLD_{max} > 1000$ m depth).

The time evolution of mean winter salinities (Figure 3d) shows a different behavior throughout the water column, showing a slightly freshening trend in MAW and a notable salinization in LIW and the 600-1000 m layer (Table S2).

The yearly SI at 1000 m depth shows values close to minimum values during the projected DWF events (Figure 3e), which suggests a weaker stratification of the water column. Until 2040s the SI does not show any significant trend. However, from 2040 the SI displays an upward trend ($0.02 \text{ m}^2\text{s}^{-2}\text{y}^{-1}$) reaching values up to $1.9 \text{ m}^2\text{s}^{-2}$ at the end of the 21st century. Therefore, the climate change signal introduced by RCP8.5 leads to a higher stratification of the water column which may hamper the formation of deep waters.

3.4 Fluxes at Gibraltar Strait

The simulated water, heat and salt exchange flows through the Strait of Gibraltar are summarized in Table 1. The water outflow in Gibraltar during 2070-2099 (period without DWF episodes) experiences a decrease of 0.04 Sv in comparison with 2006-2041 (period with DWF events), while the net water flow increases by 0.02 Sv. The heat outflux increases $2.6 \cdot 10^{10} \text{ Wyr}^{-1}$ throughout the 2006-2099 period; thus, the Mediterranean Outflow (MO) becomes warmer toward the end of the century: the mean temperature of MO during 2006-2041 is 13.5°C while for the 2070-2099 is 15.2°C . Until 2041 the MO temperature does not present any significant change. However, during the 2041-2099 period the trend of MO temperature displays a sharp increase ($0.034^\circ\text{Cyr}^{-1}$, see supplementary: Figure S1).

Table 1. Mean water, heat and salt exchange fluxes, temperature and salinity of inflow and outflow waters at Gibraltar Strait for 2006-2041 and 2070-2099 periods simulated by ROM model under the RCP8.5 scenario. Trends computed from yearly means during 2006-2099. For the net transport calculation, positive values were assigned to inflows and negative to outflows.

	2006-2041	2070-2099	Trend 2006-2099
Water inflow (Sv)	0.544	0.532	$-1.3 \cdot 10^{-4} \text{ Sv yr}^{-1}$
Water outflow (Sv)	0.507	0.476	$-4.2 \cdot 10^{-4} \text{ Sv yr}^{-1}$
Net water flow (Sv)	$3.7 \cdot 10^{-2}$	$5.6 \cdot 10^{-2}$	$3.0 \cdot 10^{-4} \text{ Sv yr}^{-1}$
Heat influx (W)	$3.17 \cdot 10^{13}$	$3.20 \cdot 10^{13}$	$0.7 \cdot 10^{10} \text{ W yr}^{-1}$
Heat outflux (W)	$2.73 \cdot 10^{13}$	$2.88 \cdot 10^{13}$	$2.6 \cdot 10^{10} \text{ W yr}^{-1}$
Net heat transport (W)	$4.4 \cdot 10^{12}$	$3.2 \cdot 10^{12}$	$-1.9 \cdot 10^{10} \text{ W yr}^{-1}$
Salt influx (kg s^{-1})	$1.68 \cdot 10^7$	$1.65 \cdot 10^7$	$-3.4 \cdot 10^3 \text{ kg s}^{-1} \text{ yr}^{-1}$
Salt outflux (kg s^{-1})	$1.80 \cdot 10^7$	$1.72 \cdot 10^7$	$-1.1 \cdot 10^4 \text{ kg s}^{-1} \text{ yr}^{-1}$
Net salt transport (kg s^{-1})	$-1.2 \cdot 10^6$	$-7.0 \cdot 10^5$	$7.1 \cdot 10^3 \text{ kg s}^{-1} \text{ yr}^{-1}$
Temperature of inflow waters ($^\circ\text{C}$)	16.0	16.3	$4.8 \cdot 10^{-3} \text{ }^\circ\text{C yr}^{-1}$
Temperature of outflow waters ($^\circ\text{C}$)	13.5	15.2	$2.6 \cdot 10^{-2} \text{ }^\circ\text{C yr}^{-1}$
Salinity of inflow waters (psu)	36.3	35.8	$-9.0 \cdot 10^{-3} \text{ psu yr}^{-1}$
Salinity of outflow waters (psu)	38.1	38.2	$2.0 \cdot 10^{-3} \text{ psu yr}^{-1}$

The salinity of the inflow in Gibraltar decreases ($-9.0 \cdot 10^{-3} \text{ psuyr}^{-1}$) due to the freshening of the inflowing Atlantic waters. This fresher Atlantic water is the main contributor to the surface freshening in the GoL. Otherwise, the outflow waters become saltier ($+2.0 \cdot 10^{-3} \text{ psuyr}^{-1}$) because of the salinization of LIW and deeper waters as shown in Figure 3, thus the salt transport through the Strait to Atlantic Ocean increases (Table 1).

4 Discussion and Conclusions

The response of the NWMed deep water formation to climate change has been explored in Soto-Navarro et al. (2020). The authors found in an ensemble of six Regional Climate Models a robust dramatic decrease of DWF by the end of the 21st century. However, the mechanisms involved were not revealed. As the time evolution of the DWF is strongly model dependent, single model runs can be used to identify in a physically consistent way the causes of this collapse. Therefore, we study these mechanisms in one of the simulations used in Soto-Navarro et al. (2020). Specifically, we analyze the simulation with the regionally coupled system ROM under the RCP8.5 scenario.

Our simulation is able to reproduce the several DWF episodes during the present period: deep convection occurs every year from 2009 to 2014 (Figure 2a and Table S1), what is statistically in good agreement with observations (Houpert et al., 2016; Somot et al., 2018; Margirier et al., 2020).

Starting from the early 2040s, we find a dramatic reduction of MLD_{max} in the GoL (Figure 2a). The maximum MLD for the present climate (1976-2005) is $2385 \pm 630 \text{ m}$ while for 2070-2099 under the RCP8.5 scenario is $297 \pm 47 \text{ m}$. That is, the MLD_{max} simulated by ROM experiences a reduction of almost 90% in the GoL. These values are in close agreement with values reported in Soto-Navarro et al. (2020).

Exploring the possible mechanisms (t. e. air-sea fluxes and ocean preconditioning) that lead to this dramatic MLD_{max} decrease we find that the air-sea fluxes do not seem to be the factor responsible for the DWF collapse, as the buoyancy loss does not change significantly (Figure 2b). Changes in the buoyancy loss also cannot explain the changes in DWF strength, as strong or weak DWF events can happen with similar BL values. In agreement with Somot et al. (2018), our results show that in any case no deep water is formed ($\text{MLD}_{\text{max}} < 1000 \text{ m}$) when $\text{BL} < 0.6 \text{ m}^2\text{s}^{-2}$ during the 2006-2013 period.

Our results indicate that the changes in properties of the upper and intermediate water masses affecting the ocean preconditioning are key in the DWF collapse. In our simulation, the temperatures of MAW and LIW are projected to increase 2.6°C and 2.3°C , respectively (Figure 3a and 3b). In turn, the salinity decreases slightly (-0.01 psu) on the surface, while deeper waters become saltier (Figure 3c and 3d). As shown previously in Parras-Berrocal et al. (2020), the warming and freshening signal of MAW comes to the GoL from the Eastern Atlantic, while the increase of LIW temperature and salinity is propagated from its formation area in the Eastern Mediterranean. These changes increase the vertical

density gradient between the MAW and LIW, strongly reducing the vertical mixing between these water masses. This is reflected in the stratification index for the 0-1000 m water column (Figure 3e), which from 2040s onward experiences a positive trend ($0.02 \text{ m}^2\text{s}^{-2}\text{y}^{-1}$). Our results do not show a significant change in atmospheric fluxes, changes in MAW and LIW characteristics play the main role in the DWF collapse in the NWMed. The recent study of Margirier et al. (2020) lends some support to our hypothesis: they found in glider and other platforms profiles collected over 2007-2017 that an abrupt jump of LIW temperature and salinity provoked a strong reduction of vertical mixing in the NWMed in 2014. The authors concluded that under those conditions, stronger atmospheric forcing is needed to trigger deep convection. Amitai et al. (2021) have also recently demonstrated that LIW characteristics play a key role in enabling or disabling the deep convection in the GoL. In agreement with Margirier et al. (2020) and Amitai et al. (2021), our results indicate that the projected deep water formation collapse in the 21st century is controlled by the change in LIW characteristics, but we found also that changes in MAW properties play a role. In order to assess the relative contribution of LIW and MAW to the deep water formation collapse we compare the SI calculated from spatially and temporally averaged vertical profiles in the GoL in four cases (Figure S2): (i) using the values corresponding to the pre-collapse period (2006-2041); (ii) using the values corresponding to the post-collapse period (2070-2099); and creating additionally two synthetic profiles, (iii) one containing the pre-collapse characteristics of MAW (0-200 m depth) with the post-collapse properties of deeper layers (200-1000 m depth; Figure S2g), and (iv) a second one with the post-collapse MAW and pre-collapse deeper layers. As seen in Figure S2, there is a clear increase in the post-collapse SI (see also Fig. 3e), but interestingly the SI for the (iv) situation ($1.20 \text{ m}^2\text{s}^{-2}$, Figure S2h) is greater than for the (iii) ($0.97 \text{ m}^2\text{s}^{-2}$, Figure S2g). This results suggest that in the future the change in MAW properties will play a role at least as relevant as LIW in the deep water formation collapse. This collapse of NWMed deep water formation seems to have an impact on the ventilation and on the thermohaline circulation of the Mediterranean Sea.

Both inflow and outflow water transport at the Strait of Gibraltar show a decreasing trend which is larger in the outflow, increasing the net flow (Table 1). Moreover, the incoming surface Atlantic jet will transport more heat and less salt into the Mediterranean basin, causing the hydrographic changes of surface waters (MAW) in the GoL represented in Figure 3. At the same time, the salinization of intermediate (LIW) in the Mediterranean Sea contributes to the increase of MO salinity. As a result, the MO will be warmer and saltier by the end of the 21st century. During the period with DWF episodes (2006-2041) the warming of MO is gradual and does not present noticeable changes, however after the collapse of DWF it accelerates reaching an increase rate of $0.034^\circ\text{Cyr}^{-1}$ (Figure S1). Then, the collapse of DWF could be one of the driving factors of the changes in characteristics of fluxes at Gibraltar Strait which reflects changes in the Mediterranean overturning circulation at large scale.

Acknowledgments and Data

I. M. Parras-Berrocal, O. Álvarez and M. Bruno were supported by the Spanish National Research Plan through project TRUCO (RTI2018-100865-BC22). R. Vázquez was supported through a doctoral grant at the University Ferrara and University of Cádiz. W. Cabos have been funded by the Spanish Ministry of Science, Innovation and Universities, the Spanish State Research Agency and the European Regional Development Fund, through grant CGL2017-89583-R. D. Sein was supported in the framework of the state assignment of the Ministry of Science and Higher Education of Russia (0128-2021-0014). The model data are available online (at <https://doi.org/10.5281/zenodo.5151396>).

The authors declare that they have no conflict of interest.

References

- Adloff, F., Somot, S., Sevault, F., Jordà, G., Aznar, R., Déqué, M., Herrmann, M., Marcos, M., Dubois, C., Padorno, E., & Alvarez-Fanjul, E. (2015). Mediterranean Sea response to climate change in an ensemble of twenty first century scenarios. *Climate Dynamics*, 45, 2775–2802. <https://doi.org/10.1007/s00382-015-2507-3>
- Amitai, Y., Ashkenazy, Y., & Gildor, H. (2021). The Effect of the Source of Deep Water in the Eastern Mediterranean on Western Mediterranean Intermediate and Deep Water. *Frontiers in Marine Science*, 7:615975. <https://doi.org/10.3389/fmars.2020.615975>
- Bethoux, J.P., & Gentili, B. (1999). Functioning of the Mediterranean Sea: past and present changes related to freshwater input and climate changes. *Journal of Marine Systems*, 20, 33–47. [https://doi.org/10.1016/S09247963\(98\)00069-4](https://doi.org/10.1016/S09247963(98)00069-4)
- Darmaraki, S., Somot, S., Sevault, F., Nabat, P., Cabos Narvaez, W. D., Cavicchia, L., Djurdjevic, V., Li, L., Sannino, G., & Sein, D. V. (2019). Future evolution of Marine Heatwaves in the Mediterranean Sea, *Climate Dynamics*, 53, 1371–1392. <https://doi.org/10.1007/s00382-019-04661-z>
- D’Ortenzio, F., Iudicone, D., de Boyer Montegut, C., Testor, P., Antoine, D., Marullo, S., Santoreli, R., & Madec, G. (2005). Seasonal variability of the mixed layer depth in the mediterranean sea as derived from in situ profiles. *Geophysical Research Letter*, 32, L12605. <https://doi.org/10.1029/2005GL022463>
- Durrieu de Madron, X., Houpert, L., Puig, P., Sanchez-Vidal, A., Testor, P., Bosse, A., Estournel, C., Somot, S., Bourrin, F., Bouin, M. N., Beauverger, M., Beguery, L., Calafat, A., Canals, M., Cassou, C., Coppola, L., Dausse, D., D’Ortenzio, F., Font, J., Heussner, S., Kunesch, S., Lefevre, D., Goff, H. L., Martin, J., Mortier, L., Palanques, A., & Raimbault, P. (2013). Interaction of dense shelf water cascading and open-sea convection in the Northwestern Mediterranean during winter 2012. *Geophysical Research Letter*, 40, 1379–1385. <https://doi.org/10.1002/grl.50331>

- Giorgetta, M. A., Jungclauss, J., Reick, C. H., Legutke, S., Bader, J., Böttinger, M., Brovkin, V., Crueger, T., Esch, M., Fieg, K., Glushak, K., Gayler, V., Haak, H., Hollweg, H.-D., Ily-ina, T., Kinne, S., Kornblueh, L., Matei, D., Mauritsen, T., Mikolajewicz, U., Mueller, W., Notz, D., Pithan, F., Raddatz, T., Rast, S., Redler, R., Roeckner, E., Schmidt, H., Schnur, R., Segschneider, J., Six, K. D., Stockhause, M., Timmreck, C., Wegner, J., Widmann, H., Wieners, K.-H., Claussen, M., Marotzke, J., & Stevens, B. (2013). Climate and carbon cycle changes from 1850 to 2100 in MPI-ESM simulations for the Coupled Model Intercomparison Project phase 5. *Journal of Advances in Modelling Earth Systems*, 5, 572–597, <https://doi.org/10.1002/jame.20038>
- Giorgi, F. (2006). Climate change hot-spots. *Geophysical Research Letter*, 33, L08707. <https://doi.org/10.1029/2006GL025734>
- Hagemann, S., & Dümenil-Gates, L. (1998). A parameterization of the lateral waterflow for the global scale *Climate Dynamics*, 14, 17–31. <https://doi.org/10.1007/s003820050205>
- Hagemann, S. & Dümenil-Gates, L. (2001). Validation of the hydrological cycle of ECMWF and NCEP reanalysis using the MPI hydrological discharge model. *Journal Geophysical Research*, 106, 1503–1510. <https://doi.org/10.1029/2000JD900568>
- Herrmann, M., Sevault, F., Beuvier, J., & Somot, S. (2010). What induced the exceptional 2005 convection event in the northwestern Mediterranean basin? Answers from a modeling study. *Journal Geophysical Research: Oceans*, 115(C12)051. <https://doi.org/10.1029/2010JC006162>
- Hibler, W. D. (1979). A dynamic thermodynamic sea ice model. *Journal of Physical Oceanography*, 9, 815–846. [https://doi.org/10.1175/1520-0485\(1979\)009<0815:ADTSIM>2.0.CO;2](https://doi.org/10.1175/1520-0485(1979)009<0815:ADTSIM>2.0.CO;2)
- Houpert, L., Durrieu de Madron, X., Testor, P., Bosse, A., D’Ortenzio, F., Bouin, M. N., Dausse, D., Le Goff, H., Kunesch, S., Labaste, M., & Coppola, L. (2016). Observations of open-ocean deep convection in the northwestern Mediterranean Sea: Seasonal and interannual variability of mixing and deep water masses for the 2007-2013 period. *Journal of Geophysical Research: Oceans*, 121(11), 8139–8171. <https://doi.org/10.1002/2016JC011857>
- IPCC. (2013). *Climate Change 2013: The Physical Science Basis*. Contribution of Working Group I to the Fifth Assessment Report of the Intergovernmental Panel on Climate Change (Stocker TF, Qin D, Plattner G-K, Tignor M, Allen SK, Boschung J, Nauels A, Xia Y, Bex V and Midgley PM (eds)). Cambridge University Press, Cambridge and New York, pp 1535
- Jacob, D. (2001). A note to the simulation of the annual and interannual variability of the water budget over the Baltic Sea drainage basin. *Meteorology and Atmospheric Physics*, 77, 61–73. <https://doi.org/10.1007/s007030170017>
- Jungclauss, J. H., Fischer, N., Haak, H., Lohmann, K., Marotzke, J., Matei,

- D., Mikolajewicz, U., Notz, D., & von Storch, J. S. (2013). Characteristics of the ocean simulations in MPIOM, the ocean component of the MPI-Earth system model. *Journal of Advances in Modelling Earth Systems*, 5, 422–446. <https://doi.org/10.1002/jame.20023>
- Lascaratos, A., Williams, R., & Tragou, E. (1993). A mixed-layer study of the formation of Levantine Intermediate Water. *Journal Geophysical Research*, 98(C8), 14739–14749. <https://doi.org/10.1029/93JC00912>
- Leaman, K., & Schott, F. (1991). Hydrographic structure of the convection regime in the Gulf of Lions: Winter 1987. *Journal of Physical Oceanography*, 21(4), 575–598.
- Léger, F., Lebeaupin Brossier, C., Giordani, H., Arsouze, T., Beuvier, J., Bouin, M.-N., Bresson, E., Ducrocq, V., Fourrié, N., & Nuret, M. (2016). Dense water formation in the north- western Mediterranean area during HyMeX-SOP2 in 1/36° ocean simulations: Sensitivity to initial conditions. *Journal Geophysical Research: Oceans*, 121(8), 5549–5569. <https://doi.org/10.1002/2015JC011542>
- L’Hévéder, B. Li, L. Sevault, F. & Somot, S. (2013). Interannual variability of deep convection in the Northwestern Mediterranean simulated with a coupled AORCM. *Climate Dynamics*, 41(3–4), 937–960. <https://doi.org/10.1007/s00382-012-1527-5>
- Maier-Reimer, E., Kriest, I., Segschneider, J., & Wetzol, P. (2005). The Hamburg Ocean Carbon Cycle Model HAMOCC5.1 Technical Description Release 1.1, Ber. Erdsystemforschung, 14, available at: <http://hdl.handle.net/11858/00-001M-0000-0011-FF5C-D>
- Margirier, F., Testor, P., Heslop, E., Mallil, K., Bosse, A., Houpert, L., Mortier, L., Bouin, M.-B., Coppola, L., D’Ortenzio, F., Durrie de Madron, X., Murre, B., Prieur, L., Raimbault, P. & Taillandier, V. (2020). Abrupt warming and salinification of intermediate waters interplays with decline of deep convection in the Northwestern Mediterranean Sea. *Scientific Reports* 10, 20923. <https://doi.org/10.1038/s41598-020-77859-5>
- Marshall, J., & Schott, F. (1999). Open-ocean convection: observations, theory, and models. *Reviews of Geophysics*, 37(1), 1–64. <https://doi.org/10.1029/98RG02739>
- Marsland, S. J., Haak, H., Jungclaus, J. H., Latif, M., & Roeske, F. (2003). The Max-Planck- Institute global ocean/sea ice model with orthogonal curvilinear coordinates. *Ocean Modelling*, 5 (2), 91–127, [https://doi.org/10.1016/S1463-5003\(02\)00015-X](https://doi.org/10.1016/S1463-5003(02)00015-X)
- MEDOC Group. (1970). Observations of formation of deep-water in the Mediterranean Sea. *Nature*, 227, 1037–1040. <https://doi.org/10.1038/2271037a0>
- Menna, M. & Poulain, P. M. (2010). Mediterranean intermediate circulation estimated from Argo data in 2003–2010. *Ocean Science*, 6, 331–343. <https://doi.org/10.5194/os-6-331-2010>

- Mertens, C., & Schott, F. (1998). Interannual variability of deep-water formation in the northwestern Mediterranean. *Journal of Physical Oceanography*, 28, 1410–1423, [https://doi.org/10.1175/1520-0485\(1998\)028%3c1410:IVODWF%3e2.0.CO;2](https://doi.org/10.1175/1520-0485(1998)028%3c1410:IVODWF%3e2.0.CO;2)
- Mikolajewicz, U., Sein, D. V., Jacob, D., Königk, T., Podzun, R. & Semmler, T. (2005). Simulating Arctic sea ice variability with a coupled regional atmosphere-ocean-sea ice model. *Meteorologische Zeitschrift*, 14 (6), 793–800. <https://doi.org/10.1127/0941-2948/2005/0083>
- Millot, C. (1999). Circulation in the Western Mediterranean Sea, *Journal of Marine Systems*, 20 (1-4), 423-440. [https://doi.org/10.1016/S0924-7963\(98\)00078-5](https://doi.org/10.1016/S0924-7963(98)00078-5)
- Millot, C. (2005). Circulation in the mediterranean sea: Evidences, debates and unanswered questions, *Scientia Marina*, 69, 5–21. <https://doi.org/10.3989/scimar.2005.69s15>
- Millot, C. (2014). Levantine Intermediate Water characteristics: an astounding general misunderstanding! (addendum), *Scientia Marina*, 78(2), 165–171. <https://doi.org/10.3989/scimar.04045.30H>
- Parras-Berrocal, I. M., Vazquez, R., Cabos, W., Sein, D., Mañanes, R., Perez-Sanz, J., & Izquierdo, A. (2020). The climate change signal in the Mediterranean Sea in a regionally coupled atmosphere–ocean model, *Ocean Science*, 16, 743–765. <https://doi.org/10.5194/os-16-743-2020>
- Rechid, D., & Jacob, D.: Influence of monthly varying vegetation on the simulated climate in Europe. *Meteorologische Zeitschrift*, 15(1), 99–116. <https://doi.org/10.1127/0941-2948/2006/0091>
- Rhein, M. (1995). Deep water formation in western Mediterranean. *Journal of Geophysical Research*, 100-C4, 6943-6959. <https://doi.org/10.1029/94JC03198>
- Robinson, A., Leslie, W., Theocharis, A., & Lascaratos, A. (2001). *Encyclopedia of ocean sciences*. Academic Press Ltd., London chap Mediterranean Sea Circulation
- Sánchez-Gómez, E., Somot, S., Josey, S. A., Dubois, C., Elguindi, N., & Déqué, M. (2011). Evaluation of Mediterranean Sea water and heat budgets simulated by an ensemble of high resolution regional climate models. *Climate Dynamics*, 37, 2067–2086. <https://doi.org/10.1007/s00382-011-1012-6>
- Schott, F., & Leaman, K. D. (1991). Observations with Moored Acoustic Doppler Current Profilers in the Convection Regime in the Golfe du Lion. *Journal of Physical Oceanography*, 21, 558–574, [https://doi.org/10.1175/1520-0485\(1991\)021<0558:OWMADC>2.0.CO;2](https://doi.org/10.1175/1520-0485(1991)021<0558:OWMADC>2.0.CO;2)
- Sein, D. V., Mikolajewicz, U., Gröger, M., Fast, I., Cabos, W., Pinto, J. G., Hagemann, S., Semmler, T., Izquierdo, A., & Jacob, D. (2015). Regionally coupled atmosphere-ocean- sea ice-marine biogeochemistry model ROM: 1. Description and validation, *Journal of Advance in Modelling Earth Systems*, 7(1),

268–304. <https://doi.org/10.1002/2014MS000357>

Sein, D. V., Gröger, M., Cabos, W., Alvarez-Garcia, F. J., Hagemann, S., Pinto, J. G., Izquierdo, A., de la Vara, A., Koldunov, N. V., Dvornikov, A. Y., Limareva, N., Alekseeva, E., Martinez-Lopez, B. & Jacob, D. (2020). Regionally coupled atmosphere-ocean-sea ice-marine biogeochemistry model ROM: 2. Studying the Climate Change Signal in the North Atlantic and Europe, *Journal of Advance in Modelling Earth Systems*, 12, e2019MS001646. <https://doi.org/10.1029/2019Ms001646>

Seyfried, L., Marsaleix, P., Richard, E., & Estournel, C. (2017). Modelling deep-water formation in the north-west Mediterranean Sea with a new air-sea coupled model: sensitivity to turbulent flux parameterizations. *Ocean Science*, 13, 1093–1112. <https://doi.org/10.5194/os-13-1093-2017>

Shaltout, M., & Omstedt, A. (2014). Recent sea surface temperature trends and future scenarios for the Mediterranean Sea. *Oceanologia*, 56, 411–443. <https://doi.org/10.5697/oc.56-3.411>

Somot, S., Sevault, F., & Déqué, M. (2006). Transient climate change scenario simulation of the Mediterranean Sea for the 21st century using a high-resolution ocean circulation model. *Climate Dynamics*, 27, 851–879. <https://doi.org/10.1007/s00382-006-0167-z>

Somot, S., Sevault, F., Déqué, M., & Crépon, M. (2008). 21st century climate change scenario for the Mediterranean using a coupled atmosphere-ocean regional climate model. *Global Planetary Change*, 63, 112–126. <https://doi.org/10.1016/j.gloplacha.2007.10.003>

Somot, S., Houpert, L., Sevault, F., Testor, P., Bosse, A., Taupier-Letage, I., Bouin, M. N., Waldman, R., Cassou, C., Sanchez-Gomez, E., Durrieu de Madron, X., Adloff, F., Nabat, P. & Herrman, M. (2018). Characterizing, modelling and understanding the climate variability of the deep water formation in the North-Western Mediterranean Sea. *Climate Dynamics*, 51, 1179–1210. <https://doi.org/10.1007/s00382-016-3295-0>

Soto-Navarro, J., Jordá, G., Amores, A., Cabos, W., Somot, S., Sevault, F., Macias, D., Djurdjevic, V., Sannino, G., Li, L. & Sein, D. (2020). Evolution of Mediterranean Sea water properties under climate change scenarios in the Med-CORDEX ensemble. *Climate Dynamics*, 54, 2135–2165. <https://doi.org/10.1007/s00382-019-05105-4>

Taylor, K., Stouffer, R., & Meehl, G. (2012). An overview of CMIP5 and the experiments design. *Bulletin of the American Meteorological Society*, 93, 485–498. <https://doi.org/10.1175/BAMS-D-11-00094.1>

Valcke, S. (2013). The OASIS3 coupler: a European climate modelling community software. *Geoscientific Model Development*, 6, 373–388. <https://doi.org/10.5194/gmd-6-373-2013>

Turner, J. (1973). *Buoyancy effects in fluids: Cambridge monographs on mechanics and applied mathematics*. Cambridge University Press, Cambridge

Vargas-Yáñez, M., Zunino, P., Schroeder, K., López-Jurado, J. L., Plaza, F., Serra, M., Castro, C., García-Martínez, M. C., Moya, F. & Salat, J. (2012). Extreme Western Intermediate Water formation in winter 2010. *Journal of Marine Systems*, 105-10, 52-59. <https://doi.org/10.1016/j.jmarsys.2012.05.010>

Waldman, R., Somot, S., Herrmann, M., Bosse, A., Caniaux, G., Estournel, C., Houpert, L., Prieur, L., Sevault, F., & Testor, P. (2017). Modelling the intense 2012–2013 dense water formation event in the northwestern Mediterranean Sea: Evaluation with an ensemble a simulation approach. *Journal of Geophysical Research: Oceans*, 122, 1297–1324. <https://doi.org/10.1002/2016JC012437>

Waldman, R., Somot, S., Herrmann, M., Sevault, F., & Isachsen, P. E. (2018). On the Chaotic Variability of Deep Convection in the Mediterranean Sea. *Geophysical Research Letters*, 45,2433-2443. <https://doi.org/10.1002/2017GL076319>

Wetzel, P., Haak, H., Jungclaus, J., & Maier-Reimer, E. (2004). The Max-Planck-institute global ocean/sea ice model. Model MPI-OM Technical report. http://www.mpimet.mpg.de/fileadmin/models/MPIOM/DRAFT_MPIOM_TECHNICAL_REPORT.pdf

Geophysical Research Letters

Supporting Information for

Will deep water formation collapse in the North Western Mediterranean Sea by the end of the 21st century?

Iván M. Parras-Berrocal¹, Rubén Vázquez¹, William Cabos², Dimitry V. Sein³, Oscar Álvarez¹, Miguel Bruno¹ and Alfredo Izquierdo¹

¹Instituto Universitario de Investigación Marina (INMAR), University of Cádiz, Puerto Real, Cádiz, 11510, Spain.

²Departamento de Física y Matemáticas, Universidad de Alcalá, Madrid, 28801, Spain.

³Alfred Wegener Institute for Polar and Marine Research, Bremerhaven, Germany.

Corresponding author: Iván M. Parras-Berrocal (ivan.parras@uca.es)

Contents of this file

Figures S1 to S2
Tables S1 to S2

Introduction

This supporting information contains additional figures and tables that help support the conclusions made in the main manuscript with more details.

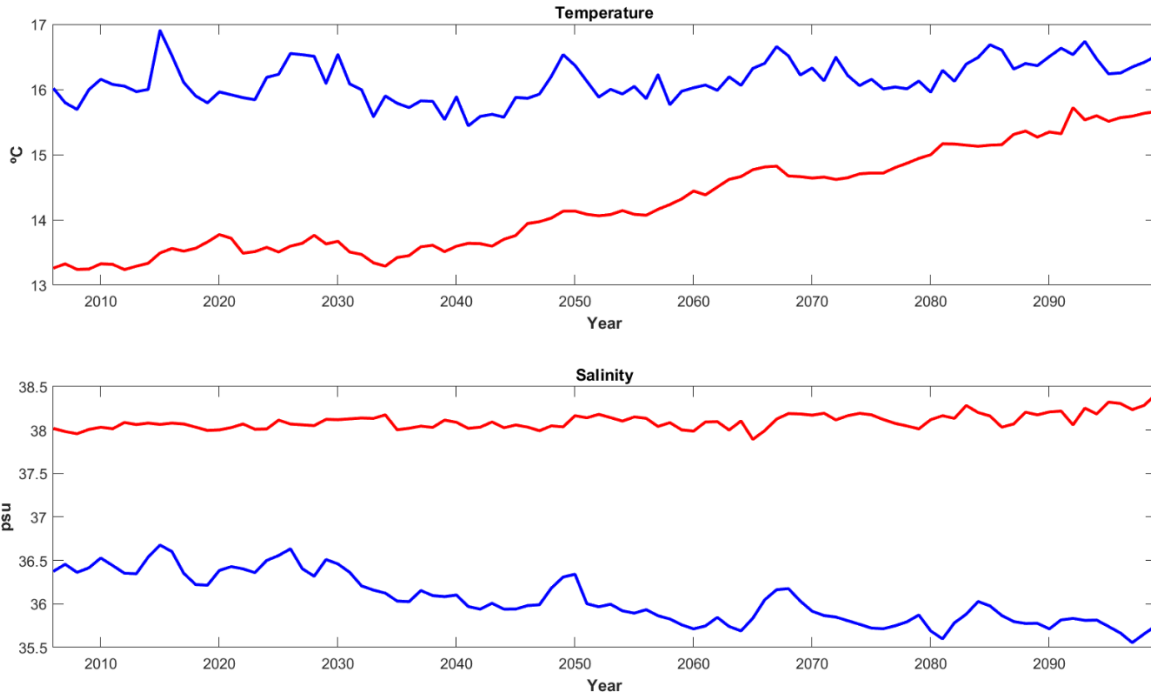


Figure S1. Interannual time series (2006-2099) of a) temperature and b) salinity inflow and outflow waters at Gibraltar Strait under RCP8.5 scenario.

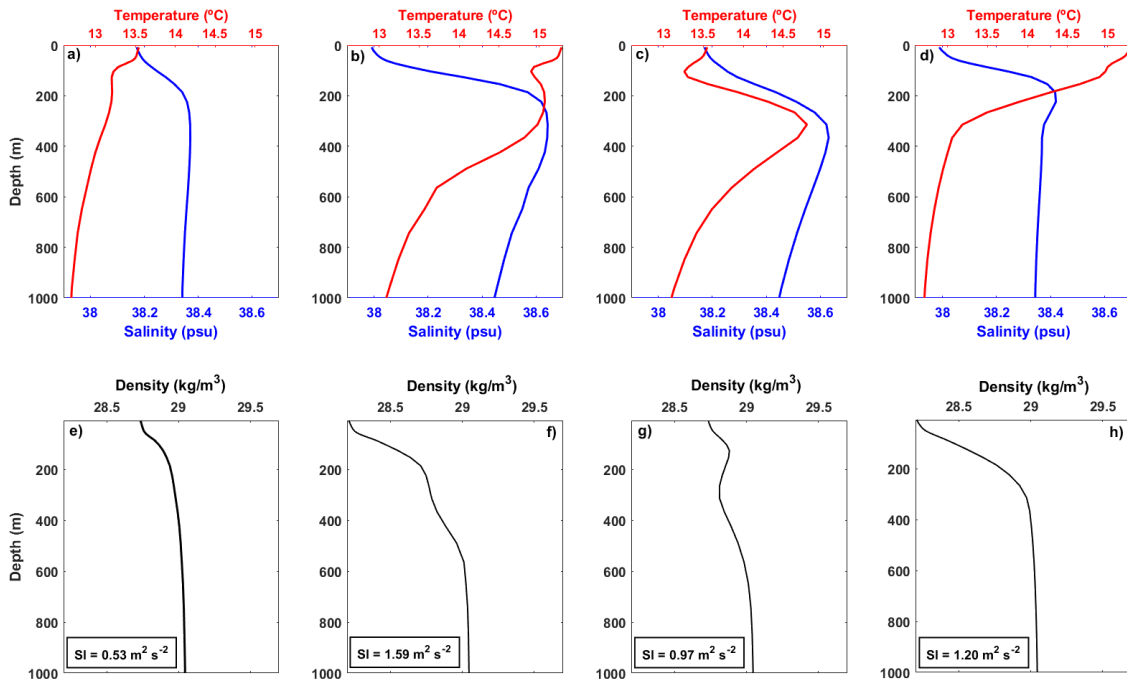


Figure S2. Spatially and temporally averaged vertical profiles of temperature, salinity and density in the GoL values corresponding to the (a, e) pre-collapse period (2006-2041), (b, f) post-collapse period (2070-2099), (c, g) pre-collapse period with characteristics of MAW (0-200 m depth) and the post-collapse period with properties of deeper layers (200-1000

m depth) and (d, h) post-collapse MAW and pre-collapse deeper layers. It is shown the stratification index (m^2s^{-2}) for each case (e, f, g, h).

Years	2009	2010	2011	2012	2013	2014	2021	2029	2031	2032	2033	2034	2037	2040	2041
MLD_{max} (m)	1589	1518	1802	1506	1229	1978	1244	1294	2126	1627	2122	1216	1043	1037	1238

Table S1. Maximum MLD for convective years simulated by ROM in the GoL for the 2006-2099 period.

	Temperature ($^{\circ}C \cdot yr^{-1}$)	Salinity ($psu \cdot r^{-1}$)
0–200 m	+0.028	$-1.5 \cdot 10^{-4}$
200–600 m	+0.024	$+4.1 \cdot 10^{-3}$
600–1000 m	+0.008	$+2.1 \cdot 10^{-3}$

Table S2. Trend computed from yearly winter means of temperature ($^{\circ}C \cdot yr^{-1}$) and salinity ($psu \cdot yr^{-1}$) computed for 4 layers (0–200 m, 200–600 m, 600–1000 m, 1000m–bottom) by ROM model in the GoL for the 2006–2099 period.